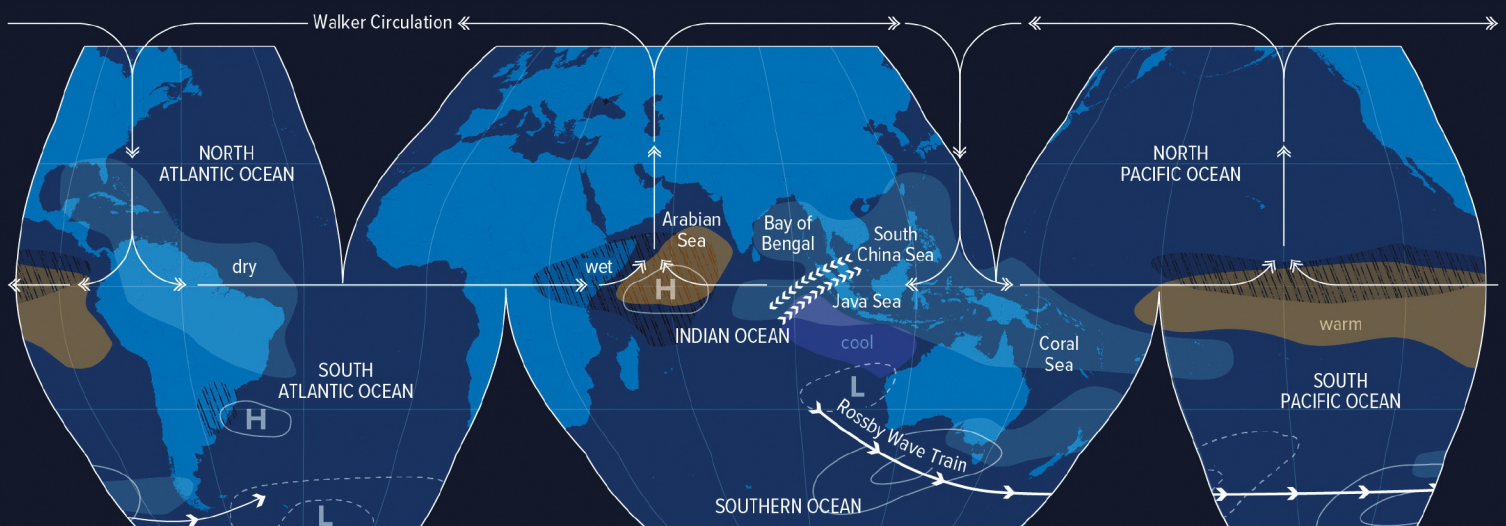
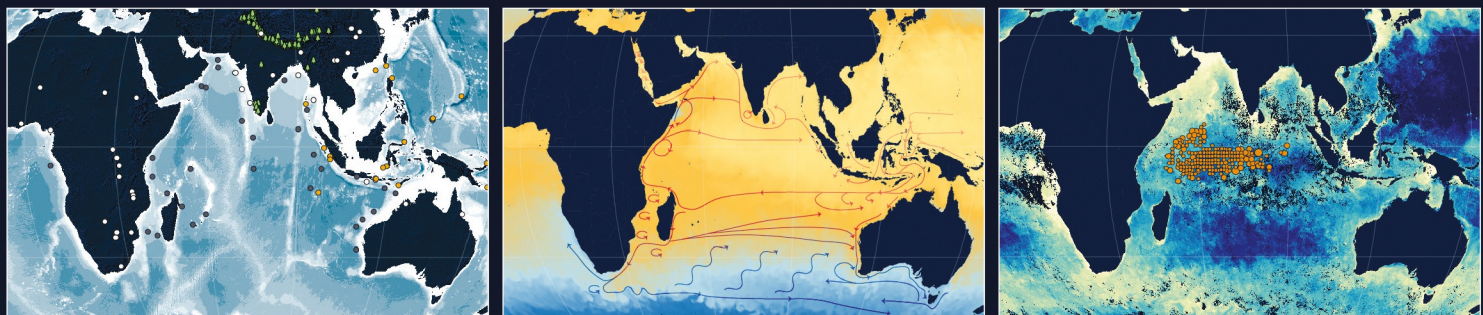


# The Indian Ocean and its Role in the Global Climate System

*Edited by Caroline C. Ummenhofer and Raleigh R. Hood*



## Chapter 18

# Modeling the Indian Ocean

Toshiaki Shinoda<sup>a</sup>, Tommy G. Jensen<sup>b</sup>, Zouhair Lachkar<sup>c</sup>, Yukio Masumoto<sup>d</sup>, and Hyodae Seo<sup>e</sup>

<sup>a</sup>*Department of Physical and Environmental Sciences, Texas A&M University-Corpus Christi, Corpus Christi, TX, United States*, <sup>b</sup>*Ocean Sciences Division, US Naval Research Laboratory, Stennis Space Center, MS, United States*, <sup>c</sup>*Arabian Center for Climate and Environmental Sciences, New York University Abu Dhabi, Abu Dhabi, United Arab Emirates*, <sup>d</sup>*Department of Earth and Planetary Science, University of Tokyo, Tokyo, Japan*, <sup>e</sup>*Department of Physical Oceanography, Woods Hole Oceanographic Institution, Woods Hole, MA, United States*

## 1 Introduction

Over the last few decades, the critical roles of the Indian Ocean in global climate variability have been recognized in climate research community (Ummenhofer et al., 2024b; Yamagata et al., 2024). Hence, the Indian Ocean is becoming one of the focus regions in the modeling community since the accurate representation of oceanic and atmospheric phenomena over the Indian Ocean in models is crucial for predicting weather and climate in many regions over the globe. Accordingly, the performance of global climate models over the Indian Ocean has begun to be evaluated, and many modeling studies that focus on examining physical processes in the Indian Ocean have been reported.

Because of the unique features of the Indian Ocean, accurate simulations of upper-ocean currents, temperature, and salinity have been a major challenge. For example, due to strong monsoons, the ocean circulation including strong western boundary currents (e.g., Somali Current) varies substantially with season. Also, a huge river discharge associated with heavy precipitation during the summer monsoon season generates very strong salinity stratification in the Bay of Bengal, resulting in a large upper ocean salinity contrast between the eastern and western portions of the basin. Unlike the eastern boundaries of other ocean basins, the boundary current along the southeast Indian Ocean (Leeuwin Current) flows poleward against the prevailing equatorward surface winds. Simulations of these unique features by large-scale ocean general circulation models have been substantially improved in recent years due primarily to the use of eddy-resolving horizontal grid scale (1/10° or finer).

Given the importance of air-sea coupled processes over the Indian Ocean for climate variability, ocean-atmosphere coupled models have been widely used recently for identifying key processes. For example, because of the improvement of global coupled general circulation models (GCMs), they have been used for examining interbasin interaction of climate variability such as the impact of the Indian Ocean Dipole (IOD) on other ocean basins. Also, regional coupled models are shown to be useful for examining a variety of air-sea feedback processes over the Indian Ocean such as the complex air-sea-land interaction over the maritime continent (Hood et al., 2024b).

Predicting marine ecosystem state over the Indian Ocean has been receiving increasing attention because of the socio-economic and environmental importance. Both regional and global ecosystem models have been used to study a variety of biogeochemical and ecological processes that are unique and highly diverse. Yet accurate simulations of various characteristics in the Indian Ocean such as large oxygen minimum zones (OMZs) have been a major challenge due to the complex interaction between physical and biogeochemical processes.

This chapter primarily covers the topics described above including the simulation of Indian Ocean circulation and upper-ocean processes by regional and global ocean models, the simulation and prediction of climate variability over the Indian Ocean, and modeling of biogeochemical processes. In addition, regional coupled modeling over the Indian Ocean, which provides a useful tool for understanding air-sea coupled processes, is discussed in a separate section. Because of the broad scope in Indian Ocean modeling, this chapter cannot fully cover all aspects of modeling. Some of the topics that are not covered in this chapter are found in other chapters, including the decadal prediction (Roxy et al., 2024; Tozuka et al., 2024), intraseasonal variability and prediction (DeMott et al., 2024), and modeling of monsoons (Ummenhofer et al., 2024a).

---

<sup>®</sup>This book has a companion website hosting complementary materials. Visit this URL to access it: <https://www.elsevier.com/books-and-journals/book-companion/9780128226988>.

## 2 Ocean circulation and upper-ocean structure

In this section, upper-ocean circulation and structure simulated by regional and global models as well as physical and dynamical processes identified based on the modeling or model/data comparisons are discussed.

### 2.1 Boundary currents

#### 2.1.1 Somali Current

The annual reversal of monsoon winds causes a reversal of the currents north of the equator, including the strong western boundary current, the Somali Current (Fig. 4 in Phillips et al., 2024). The Somali Current reverses flow direction from an intense, deep northward flow during boreal summer with a transport in the range of 32–42Sv (Beal et al., 2003) to a weaker shallow southward flow of about 14Sv during the Northeast Monsoon. The importance of equatorial Rossby waves in establishing the strong Somali Current during the Southwest Monsoon has been demonstrated in previous studies (e.g., Beal & Donohue, 2013; Lighthill, 1969; McCreary et al., 1993). The onset of northward flow in the Somali Current starts in April nearly 2 months before the onset of southerly winds, which is attributed to the arrival of Rossby waves (Beal & Donohue, 2013).

During boreal summer, the Somali Current is associated with a large anticyclonic eddy off the coast of Somalia, known as the Great Whirl (e.g., Beal & Donohue, 2013; Melzer et al., 2019; Schott & McCreary, 2001; Schott et al., 1990). The persistence of the Great Whirl during boreal fall has been shown to contribute to the existence of northward flow in the northern part of Somail Current after the weakening of local southwesterly winds (e.g., Quadfasel, 1982; Wang et al., 2018). The generation mechanism of the Great Whirl has been investigated by regional ocean models. Proposed mechanisms of the generation include local wind stress curl (McCreary & Kundu, 1985), inertial instability due to crossing the equator (Anderson & Moore, 1979), and barotropic instability (Jensen, 1991).

During July and August, the cross-equatorial Southern Gyre migrates northward (Swallow & Fieux, 1982) and merges with the Great Whirl. Cyclonic eddies often appear on the eastern flank of the Great Whirl and south of the Socotra Eddy and are advected clockwise around the Great Whirl (Beal & Donohue, 2013; Jensen, 1991). Such northward migration has been simulated by a high-resolution (3.5 km) regional coupled model (Chen et al., 2010; Hodur, 1997) (Fig. 1). In this simulation, an intense cyclonic eddy is shredded and subsequently absorbed into the Great Whirl. This process increases the potential vorticity of the anti-cyclonic Great Whirl and permits it to migrate northward. The annual reversal of the Somali Current has been well simulated by a high-resolution (0.1°) global ocean GCM and the important role of the Great Whirl and Rossby waves in the Somali Current seasonal cycle was demonstrated by the analysis of the model output (Wang et al., 2018).

#### 2.1.2 Agulhas Current

The Agulhas Current is part of the surface pathway of the global conveyor belt, flowing southward from 27°S to 40°S with a transport of 67–77 Sv (Beal et al., 2015; Beal & Bryden, 1999; Bryden et al., 2005; Gordon, 1985; Lutjeharms, 2006). The Agulhas Current is fed from the South Equatorial Current via the Mozambique Current and the East Madagascar Current. A notable feature of the Agulhas Current is a retroflexion south of Africa near 18°E. Large cyclonic meanders, known as Natal pulses, appear on the Agulhas Current southern edge. They play a significant role in the generation of Agulhas rings that enter the South Atlantic Ocean and transport significant volumes of warm and saline water. While the Agulhas Current retroflexion is difficult to represent well in most models even at high resolution (e.g., Thoppil et al., 2011), a recent study by Biastoch et al. (2018) demonstrated that a global ocean GCM with an unstructured-mesh grid (~8 km spacing in the AC region) was able to simulate the Agulhas Current, including its retroflexion, reasonably well. Renault et al. (2017) pointed out the importance of including the ocean current in the momentum flux exchange between air and sea to reduce the eddy kinetic energy (EKE) in the Agulhas Current system so that it is closer to observations, and they demonstrated improvement of AC simulation in a coupled atmosphere-ocean model.

#### 2.1.3 Leeuwin Current

The Leeuwin Current is an eastern boundary current in the southeast Indian Ocean, which flows along the west coast of Australia (Fig. 9 in Phillips et al., 2024). Among eastern boundary currents, it is unique as its near-surface water (0–250 m) flows poleward against the prevailing winds (Church et al., 1989; Cresswell & Golding, 1980). The transport is about 1.4 Sv in February and 6.8 Sv in June, while the Leeuwin Undercurrent (250–800 m at 30°S) flows equatorward with a transport of about 5 Sv (Smith et al., 1991). Variability of the Leeuwin Current strongly impacts regional climate variability such as the Ningaloo Niño (e.g., Feng et al., 2013, 2023, 2024; Yamagata et al., 2024) and local marine ecosystems (e.g., Pearce & Feng, 2013; Wernberg et al., 2013).

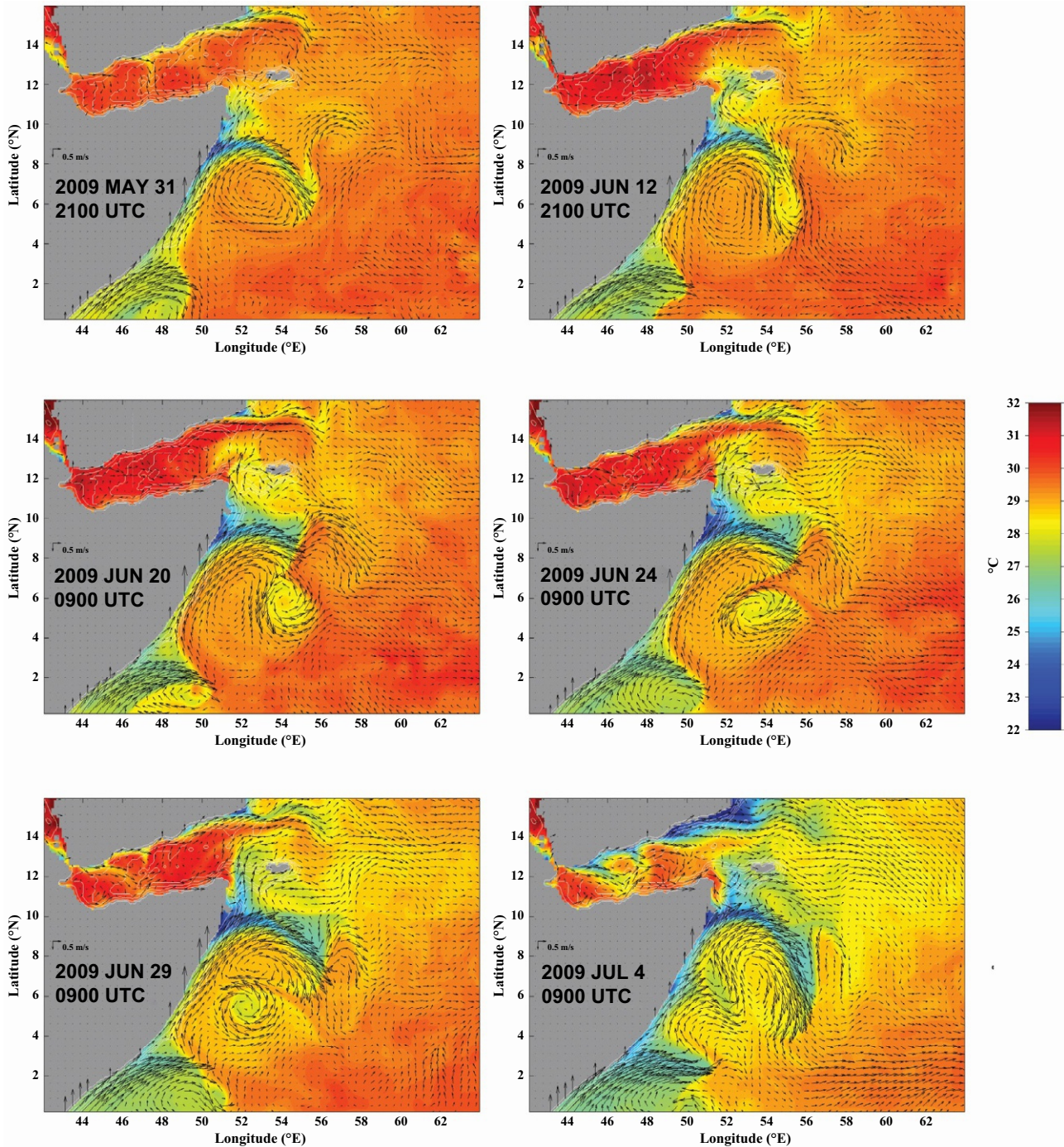


**FIG. 1** Cyclonic eddy generation in the outflow region of the upwelling wedge on the western edge of the Great Whirl in a high-resolution fully coupled regional atmosphere-ocean-wave model. The color shading and arrows show sea surface temperature and surface currents, respectively. The observational data are assimilated in the atmospheric component only.

Accurate simulation of the Leeuwin Current in large-scale ocean models has been a challenge due partly to its narrow width (30–50 km). Because of the recent development of high-resolution ocean models, some of the global ocean GCMs are able to realistically simulate the Leeuwin Current. For example, a global ocean GCM with a grid spacing of  $1/10^\circ$  was able to reproduce the Leeuwin Current with the strength ( $\sim 30$ – $50$  cm/s) and the seasonal cycle estimated from hydrographic observations (Furue, 2019). The model also generated the Leeuwin Undercurrent that flows northward around 300–500 m. However, the simulated undercurrent was weaker and almost vanishes north of  $22^\circ\text{S}$  where a strong Leeuwin Undercurrent is observed.

## 2.2 Equatorial currents

During the transitions between the monsoons in boreal spring and summer, intense eastward jets appear along the equator. These jets are known as Wyrtki Jets (Wyrtki, 1973). Numerical models (Han et al., 1999; Jensen, 1993; Nagura & McPhaden, 2010) have been used to examine the generation mechanism of Wyrtki Jets, showing that the semiannual jets are strong due to an equatorial basin-resonance of the second vertical baroclinic mode (Cane & Moore, 1981; Gent, 1981). The basin-mode is a combined oscillatory mode of eastward propagating equatorial Kelvin waves with a speed of about 1.5 m/s, and westward propagating equatorial Rossby waves with one third of that speed.

While the seasonal change of the monsoons forces the semiannual Wyrtki Jets, zonal wind bursts on the equator drive intermittent surface jets as explained by Yoshida (1959). For example, when an intense Madden-Julian Oscillation (MJO) occurred in November 2011, a rapidly intensifying Yoshida Jet was generated in the central equatorial Indian Ocean with zonal currents exceeding 1 m/s in the mixed layer. The jet was observed by RAMA (Research Moored Array for African-Asian-Australian Monsoon Analysis and Prediction) buoys and simulated well by models (e.g., Jensen et al., 2015; Shinoda et al., 2016). During this period, the Yoshida jet is superimposed on the seasonal Wyrtki Jets that has a subsurface local maximum between 50 and 150 m (Jensen et al., 2015).

Equatorial Undercurrent in the Indian Ocean, which is observed during boreal winter/spring (e.g., Knauss & Taft, 1964; Knox, 1974; Swallow, 1964) and summer/fall (e.g., Bruce, 1973; Reppin et al., 1999) seasons, is highly transient. The mechanisms of Equatorial Undercurrent generation and variability have been recently investigated using regional ocean GCMs (e.g., Chen et al., 2019a, 2019b), showing the importance of equatorial Rossby and Kelvin waves forced by seasonally varying zonal winds. In the western basin, the seasonal variation of the Equatorial Undercurrent is primarily controlled by directly forced Kelvin and Rossby waves, whereas reflected Rossby waves from the eastern boundary largely contribute to the Equatorial Undercurrent variability in the eastern basin. Although high-resolution global ocean GCMs are able to reproduce the magnitude of the semiannual cycle of the Equatorial Undercurrent reasonably well, most models are not able to accurately simulate the timing of the peak value of current (Rahman et al., 2020).

## 2.3 Indonesian Throughflow

The Indonesian Throughflow (ITF) is an important component of the global thermohaline and wind-driven circulations carrying upper ocean waters from the Pacific to the Indian Ocean (Fig. 2 in Sprintall et al., 2024). Since the total transport of the ITF can be determined to first order by the “island rule” theory (Godfrey, 1989), ocean GCMs with coarse resolution can simulate the mean transport in agreement with observations (e.g., Lee et al., 2002; Schiller et al., 1998). However, the distribution of transport among different straits and passages cannot be accurately simulated in coarse resolution models. Recent development of high-resolution global ocean GCMs as well as comprehensive observations in the Indonesian Seas such as the International Nusantara Stratification and Transport program (Gordon et al., 2010) allow evaluation of the ability of ocean models to simulate ITF structures. It has been demonstrated that a global eddy-resolving (1/12°) ocean GCM is able to simulate net ITF transports as well as its distribution among inflow/outflow passages reasonably well when compared to observations (Metzger et al., 2010). The simulation was further improved by the higher resolution (1/25°) model (Metzger et al., 2010; Shinoda et al., 2016).

Seasonal and intraseasonal variations of the ITF are also simulated well by global ocean GCMs where remotely forced equatorial waves from the Indian and Pacific Oceans and local wind forcing over the Indonesian Seas determine the transport (e.g., Shinoda et al., 2012, 2016). Simulating interannual/decadal variations of the ITF structure is still a major challenge. Long integrations of global ocean GCMs have begun in recent years (e.g., Sasaki et al., 2018) but long-term in situ measurements of currents are unavailable in most areas. Sustained measurements in most major straits in the Indonesian Seas are necessary to validate the simulated long-term ITF variability.

## 2.4 Temperature and salinity upper-ocean structure

One of the notable characteristics of the upper ocean structure in the tropical Indian Ocean is the dome-like feature of the main thermocline located around 2°S-10°S in the western portion of the basin. This area of shallow thermocline is often referred to as the Seychelles-Chagos thermocline ridge (SCTR). The SCTR is maintained primarily by strong Ekman pumping due to the northward weakening of the southeast trades (McCreary et al., 1993; Xie et al., 2002). Because of the shallow mixed layer and thermocline, subseasonal to interannual sea surface temperature (SST) signals and air-sea interaction are strong in the SCTR region (e.g., Han et al., 2007; Saji et al., 2006; Xie et al., 2002) and play an important role in the generation of atmospheric convection associated with the MJO and IOD.

Ocean GCMs with coarse resolutions can simulate SCTR variability at least qualitatively (e.g., [Masumoto & Meyers, 1998](#); [Murtugudde & Busalacchi, 1999](#)). Models suggest that several processes impact SCTR variability: One ocean GCM showed that it is primarily controlled by local Ekman pumping ([Yokoi et al., 2008](#)) while others imply that the annual cycle is due to complex interactions between the response to local and remote forcing ([Hermes & Reason, 2008](#); [Nyadjro et al., 2017](#)). The relative importance of surface heat fluxes and ocean dynamics in controlling subseasonal SST variability over the SCTR is still unclear and results vary substantially between different modeling studies ([Duvel et al., 2004](#); [Halkides et al., 2015](#); [Han et al., 2007](#); [Jayakumar et al., 2011](#); [Li et al., 2014](#); [Shinoda et al., 2017](#); [Vinayachandran & Saji, 2008](#); [Yuan et al., 2020](#)).

Another unique feature of the upper ocean is found in the Bay of Bengal, where a complex stratification including a strong halocline and temperature inversion is caused by a substantial amount of freshwater input through river runoff and precipitation. In particular, the strong salinity stratification causes a shallow mixed layer and thick barrier layer (the isothermal layer below the mixed layer) (e.g., [Howden & Murtugudde, 2001](#); [Li et al., 2017a, 2017b](#); [Yu & McCreary, 2004](#)), and its accurate simulation by models is still a challenge (e.g., [Rahman et al., 2020](#)). Modeling of the upper-ocean structure of the Bay of Bengal is further discussed in [Section 4](#).

## 2.5 Future perspectives

As described in this section, ocean CGM's ability to simulate major upper ocean currents over the Indian Ocean such as western and eastern boundary currents, equatorial currents, and circulations in the Indonesian Seas have been substantially improved in recent years primarily because of the development of high-resolution (eddy-resolving) global models. Yet, the performance of ocean GCMs depends on their resolution and model physics, and the details of such model dependence are not covered in this section. A recent ocean GCM intercomparison study provides a detailed assessment of simulations from multiple state-of-the-art global ocean models ([Rahman et al., 2020](#)).

While in situ data coverage in the Indian Ocean has been improving during recent years ([Beal et al., 2020](#)), the coverage of subsurface data in many locations such as the interior southern Indian Ocean is sparse, and thus quantitative model/data comparisons are difficult. Although recent studies discuss the circulations in the southern Indian Ocean using available in situ data, numerical model outputs, and reanalysis products (e.g., [Menezes et al., 2014, 2016](#); [Nagura & McPhaden, 2018](#)), the comprehensive evaluation of model performance on different time scales is not possible at present due to the insufficient coverage of in situ observations. Hence, in addition to maintaining and enhancing the current observational network in boundary and equatorial regions, it is desirable to extend the regions of sustained observations to the data sparse areas such as the interior southern Indian Ocean for further evaluating the ocean GCM's ability to reproduce observed ocean circulations over the entire Indian Ocean ([McPhaden et al., 2024](#)).

## 3 Climate variability

### 3.1 Modeling of climate variations

The challenge of modeling climate variations in the Indian Ocean boils down to how accurately the models can reproduce the upper-ocean conditions at the intraseasonal, seasonal, interannual, and longer time scales. Early efforts to reproduce the upper-ocean variability in the Indian Ocean can be traced back to the concept of a reduced gravity model by [Lighthill \(1969\)](#). Due to the unique geographic nature of the Indian Ocean, with the northern boundary blocked by the landmass at rather a low latitude, this simple dynamical framework can successfully simulate the seasonal upper-ocean variability (e.g., [Kindle & Thompson, 1989](#); [Luther & O'Brien, 1985](#); [McCreary et al., 1993](#); [Murtugudde & Busalacchi, 1999](#)).

Efforts to simulate the three-dimensional circulations and thermohaline structures in the ocean were pioneered by [Cox \(1970, 1976\)](#), with his epoch-making work using an ocean GCM. Subsequent developments of ocean GCM simulations of the Indian Ocean make it possible to reproduce realistic ocean circulations and tracer distributions (e.g., [Godfrey & Weaver, 1991](#); [Lee & Marotzke, 1998](#)) and their variability (e.g., [Anderson & Carrington, 1993](#)).

It is natural to extend simulations to longer time-scale variations and/or incorporate air-sea coupled processes for the study of climate variations. This research direction was accelerated by the discovery and recognition of the IOD, an air-sea coupled climate variation inherent in the tropical Indian Ocean ([Saji et al., 1999](#); [Yamagata et al., 2024](#)). It is relatively easy with a modeling study to conduct quantitative analyses of processes and mechanisms involved in simulated ocean variability, and sensitivity experiments can be carried out to tease out the roles of these processes. These studies are particularly useful for examining climate variations, for which the observations are limited in terms of spatial and temporal coverages. This section briefly introduces the present status of modeling of the climate variability in the Indian Ocean, mainly focusing on the IOD (see also [Yamagata et al., 2024](#) for more discussion of the IOD).

### 3.2 Ocean dynamics

Large-scale surface wind stress variability is considered as the dominant force for the major dynamical responses associated with the climate variations. However, both local and remote responses of the upper ocean to the wind forcing need to be considered. Planetary-scale wave dynamics play a key role in this remote response.

Piece-wise investigations on processes during different phases of the IOD have been conducted, with much attention to the generation and termination periods. These studies demonstrated that equatorial Kelvin and Rossby waves play essential roles, as well as local ocean responses to the wind forcing (e.g., [Effy et al., 2020](#); [Gualdi et al., 2003](#); [Prasad & McClean, 2004](#); [Rao et al., 2007](#); [Vinayachandran et al., 2002a](#); [Wang & Yuan, 2015](#)). A major example of the remote influence can be seen for the equatorial Kelvin waves and subsequent propagation as coastal Kelvin waves along the Sumatra/Java coasts for the eastern pole of the IOD. Arrival of the upwelling (downwelling) favorable Kelvin wave at the eastern pole is associated with shallowing (deepening) of the thermocline, resulting in cooler (warmer) SST there. Atmospheric intraseasonal oscillations may also contribute to the IOD initiation and termination through Kelvin wave propagation (e.g., [Han et al., 2006](#)). Another example is westward propagating Rossby waves generated by the wind stress curl over the eastern/central Indian Ocean for the western pole of the IOD, with a similar influence on the SST variations through the vertical movement of the thermocline. However, the degree of importance of these wave dynamics to other processes such as local upwelling and surface heat flux depends on the events and regions of interest.

Coupled atmosphere-ocean general circulation models can reasonably simulate the interannual climate variations similar to the observed IOD (e.g., [Fischer et al., 2004](#); [Gualdi et al., 2003](#); [Iizuka et al., 2000](#); [Lau & Nath, 2004](#); [Song et al., 2007](#); [Wajswicz, 2004](#); [Yao et al., 2016](#)), although some biases are observed in all the models. The coupled GCMs are used for further analyses of key processes involved in the evolution of simulated IODs and for investigations on their relations to ENSO in the Pacific Ocean. For example, [Iizuka et al. \(2000\)](#) successfully reproduced the IOD characteristics and indicated that the variability in the Indian Ocean is independent of the Pacific variations. [Lau and Nath \(2004\)](#) suggested that some of the IOD-like events in their coupled GCM are associated with atmospheric teleconnection of the ENSO-related changes, while some strong IOD-like events exist with the absence of ENSO influences (see also [Yang et al., 2015](#); [Yamagata et al., 2024](#)). [Fischer et al. \(2004\)](#) suggested two possible triggers for the IOD in their coupled GCM; one is anomalously stronger southeasterly trade winds penetrated over the southeastern Indian Ocean earlier than usual, and the other is a zonal shift of the convective region over the maritime continent associated with the El Niño phenomenon in the Pacific Ocean. Other coupled GCMs also reproduced observed characteristics of the IOD events, with some of them co-occurring with ENSO events in the Pacific while some are not (e.g., [Song et al., 2007](#); [Yamagata et al., 2024](#)). These coupled GCM experiments suggest that air-sea interactions inherent in the Indian Ocean are essential for the development of the anomalous conditions, whereas there are several possibilities of the triggering processes of the IOD.

### 3.3 Heat budget analyses and salinity impacts for the IOD

Heat budget analysis has been utilized extensively, with a focus on processes responsible for changes in the SST or mixed-layer temperature for various regions and phenomena within the Indian Ocean. This is also the case for the two poles of the IOD. It has been shown that both the surface heat flux and local/remote oceanic processes are important to determine the temperature tendencies (e.g., [Delman et al., 2018](#); [Halkides & Lee, 2009](#); [Iizuka et al., 2000](#); [Thompson et al., 2009](#); [Vinayachandran et al., 2002a, 2007](#)). However, the degree of relative importance among the processes seems to be different for each target event, the region of budget analysis, and due to differences in model settings. Recent mixed-layer heat budget analysis of an eddy-resolving ocean GCM suggested the importance of the winds off the Sumatra coast to generate temperature cooling through an advective process during the positive IOD events ([Delman et al., 2018](#)). For the termination period of the positive IOD events, [Thompson et al. \(2009\)](#) showed the dominant contribution of surface heat flux in the 1997 event and ocean advective processes in 1961 and 1994 cases, whereas [Ogata and Masumoto \(2010\)](#) suggested a possible role of eddy heat transport to hasten the IOD termination in the strong events in 1994. These analyses suggest combined influences of different processes to determine the surface mixed-layer temperature variations during the IOD, which may result in relatively large uncertainty of the IOD prediction ([Tanizaki et al., 2017](#)).

An additional complication comes from salinity contributions to the upper-layer temperature and circulation variability in the tropical Indian Ocean, because of the large spatial contrasts in salinity distribution in the tropical Indian Ocean (e.g., [Kido et al., 2019a](#); [Masson et al., 2003](#); [Thompson et al., 2006](#); [Vinayachandran & Nanjundiah, 2009](#)). A series of sensitivity experiments conducted by [Kido et al. \(2019a, 2019b\)](#) demonstrated that salinity anomalies associated with the positive IOD events are generated by both the surface freshwater flux anomaly and ocean dynamical processes, particularly due to advective processes including the rectified effects of the high-frequency variability. They also showed that the salinity

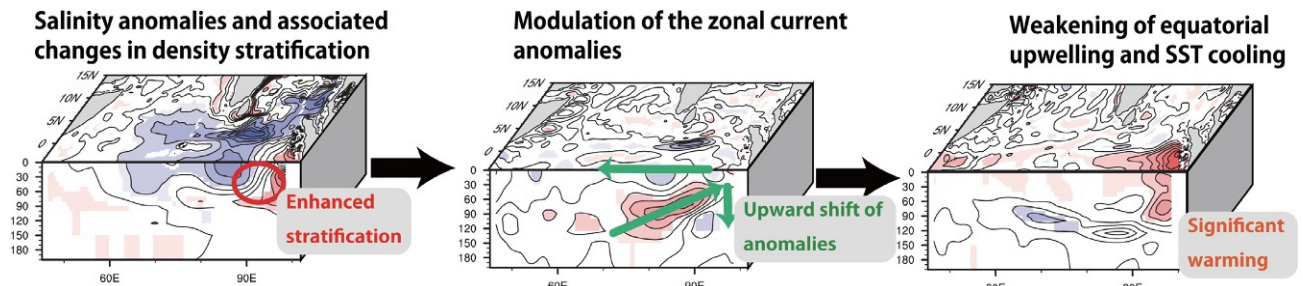


**FIG. 2** Schematic diagram showing the impact of the salinity anomaly associated with the positive IOD on the upper-ocean circulations and temperature in the equatorial Indian Ocean (see Kido et al., 2019b for details).

anomalies in turn contribute to the temperature anomaly through modification of the circulations within the vertical sections along the equator (Fig. 2).

### 3.4 Dynamical prediction of the IOD variations

Prediction and predictability studies of the IOD are important not only for scientific understanding of the phenomena but also for socioeconomic activities in surrounding regions of the Indian Ocean. Previous studies using dynamical coupled models showed reasonable prediction skill with the lead time of a few months or a season (e.g., Doi et al., 2019; Feng et al., 2014; Luo et al., 2007, 2008; Wajswicz, 2005, 2007; Yamagata et al., 2024). The potential predictability is different for the SST variability averaged over the eastern pole and western pole of the IOD, showing a shorter period of skillful prediction for the eastern pole (Wajswicz, 2005). Some of the coupled GCMs demonstrated much longer prediction skills for the IOD up to two to three seasons ahead (Lu et al., 2018; Luo et al., 2007; Song et al., 2008; Yamagata et al., 2024) in the case when anomalous conditions in the ocean played a key role in the evolution of the events. This longer prediction skill seems to come from the oceanic processes before the IOD events, such as the wave propagations, or influences from other basins, including a teleconnection from the Pacific Ocean (Doi et al., 2020; Yamagata et al., 2024).

At the same time, however, these processes may provide seeds for prediction barriers. One example of the known issues for the IOD prediction is the so-called “winter prediction barrier” (Feng et al., 2014; Wajswicz, 2007; Yamagata et al., 2024). This prediction barrier may be caused by initial errors amplified by the surface flux and/or oceanic processes (Feng et al., 2014; Feng & Duan, 2019). Doi et al. (2020) suggested that signals from the Pacific Ocean associated with the El Niño Modoki overcame the winter prediction barrier in the 2019 case. The skills for the IOD prediction may be improved by increasing model resolutions (Doi et al., 2016), initialization of subsurface ocean conditions (Doi et al., 2017), and increasing ensemble size for the prediction (Doi et al., 2019) (see Yamagata et al., 2024 for further discussion).

### 3.5 Future perspectives

The basin-scale to meso-scale variability necessary to simulate the climate variations in the Indian Ocean can be reproduced reasonably well in recent models. Air-sea coupled models and earth system models have the capability to reproduce IOD-like climate variations, showing successful prediction skills for one or two seasons ahead. Analyses of outputs from these models have highlighted important dynamical and physical processes responsible for initiation, evolution, and termination of IOD events. Our understanding of the IOD variability for individual events has been accumulated to discuss common features and differences among the events. However, further analyses of detailed mechanisms to build integrated and comprehensive pictures of the IOD and associated interactions with different time and space scales are needed.

High-resolution modeling for the purpose of process understanding is necessary to elucidate impacts from smaller-scale phenomena and boundary processes. Coordinated collaborative research will be required to do this. Analyses on long-term variability are also necessary to explore relations and interactions with longer time-scale phenomena, such as decadal variations and global warming trends. This can be achieved partly by analyzing CMIP (Coupled Model Intercomparison Project) type model output and partly by conducting long-term simulations of the ocean and/or coupled atmosphere-ocean models. Finally, a better understanding of subgrid-scale variability and turbulent processes is key to improve mixing parameterizations, which are unavoidable even in much higher resolution models.

## 4 Regional coupled climate modeling

Emphasis on regional air-sea interaction is becoming an increasingly greater focus within the climate modeling communities. However, most of the current global models use horizontal and vertical scales that are often inadequate to resolve

regional and local air-sea interaction and deep convection. Such processes have begun to be investigated by regional coupled climate models, dynamically downscaling global analyses, or coarse-resolution models in the atmosphere and ocean over a limited domain. Various regional coupled climate model studies in the Indian Ocean and other basins have unraveled novel coupled processes and advanced our understanding of how the oceans and air-sea interactions shape regional weather and climate (see reviews by [Giorgi, 2019](#); [Miller et al., 2017](#); [Schrum, 2017](#); [Xue et al., 2020](#)). This section offers a brief overview of the regional coupled climate model studies specifically designed for examining air-sea interaction in the Indian Ocean.

## 4.1 Processes and regions suitable for regional coupled climate model applications

### 4.1.1 Mesoscale air-sea interactions

One of the most crucial benefits of an regional coupled climate model is the improved representation of air-sea interaction mediated by ocean mesoscale eddies. Despite their small spatial scales, the mesoscale flow fields typically feature strong anomalies in SSTs and their gradients ([Chelton et al., 2007](#); [Small et al., 2008](#); [Vecchi et al., 2004](#); [Fig. 3](#)). [Seo et al. \(2008\)](#) used a 25-km regional coupled climate model ([Seo et al., 2007](#)) in the Arabian Sea to study the influence of surface wind variations on mesoscale SST variability, suggesting that the local boundary layer coupling is a vital forcing mechanism of baroclinic instability that governs the regional ocean circulation. In the Bay of Bengal, [Seo et al. \(2019\)](#) used a 4-km regional coupled climate model ([Seo et al., 2014](#)) to show how the effect of a surface current in the wind stress ([Renault et al., 2016](#); [Seo et al., 2016](#)) acts to stabilize the ocean circulation and increase the upper ocean stratification. [Seo \(2017\)](#) further conducted a series of 7-km regional coupled climate model simulations for the Arabian Sea to quantify relative impacts of the mesoscale SST-driven and current-driven wind stress responses ([Renault et al., 2019](#)), showing that the two couplings exert distinct influences on the ocean: the thermal (mechanical) coupling acts to shift the position (intensity) of the mesoscale flow fields.

### 4.1.2 Indian summer monsoons and Intraseasonal variability (ISV)

In the tropics, the local air-sea coupling is effectively communicated to the deep troposphere via their impacts on cumulus convection, leading to well-defined regional air-sea coupled effects on the Indian summer monsoon precipitation and its ISV ([DeMott et al., 2015, 2024](#)). Using regional coupled climate model simulations of [Li et al. \(2012\)](#), [Misra et al. \(2017\)](#) concluded that their 15-km model not only produces improved simulation skill in Indian summer monsoon rainfall but also accurately captured the transition of the active/break cycles of the Indian summer monsoon and remote impacts by ENSO. Theories and global modeling studies have demonstrated that local air-sea coupling is critical for realistic simulation of the northward propagating Indian summer monsoon ISV ([DeMott et al., 2013](#); [Fu et al., 2007, 2008](#)). The subsequent studies by Misra and colleagues ([Karmakar & Misra, 2020a, 2020b](#); [Misra et al., 2018](#)) have illustrated the importance of the regional air-sea interaction in the simulation of the Indian Ocean subseasonal, seasonal and interannual climate ([Fig. 4](#)).

### 4.1.3 Maritime Continent

The maritime continent is an ideal region for regional coupled climate model applications. It is the largest archipelago with complex coastlines and island geometry, surrounded by oceans of significant heat content supporting deep convection. The thermally forced diurnal convection from land migrates offshore while interacting with oceanic and land-surface processes ([Yoneyama & Zhang, 2020](#)), which are too small in scales to be reliably represented in global models and analyses ([Xue et al., 2020](#)). [Aldrian et al. \(2005\)](#) were the first to apply a regional coupled climate model to the maritime continent, identifying significant skill enhancement in rainfall as compared to uncoupled runs. [Wei et al. \(2014\)](#) demonstrated improved simulations of SST and ITF transport in their regional coupled climate model. However, they did not find the corresponding improvement in the rainfall bias, which is at odds with the recent observational and modeling studies showing significant impacts of air-sea coupling on the atmosphere. [Li et al. \(2017c\)](#) explored the resolution sensitivity of the diurnal precipitation and its land-sea characteristics in the Maritime Continent using the regional coupled climate model of [Samson et al. \(2014\)](#). They found that the mean SST and rainfall biases are reduced from  $\frac{3}{4}^{\circ}$  to  $\frac{1}{4}^{\circ}$  ocean models, but the rainfall becomes too strong in the  $1/12^{\circ}$  atmospheric model, in agreement with previous high-resolution atmospheric modeling studies ([Vincent & Lane, 2017](#)). While there are numerous contributors to the excessive precipitation bias in high-resolution models (e.g., radiation and cloud microphysics parameterizations) in the context of air-sea coupled modeling, improved representations of upper-ocean processes and air-sea fluxes, for example, due to tides and surface waves, are likely significant in the maritime continent. However, to date, there have been no regional coupled climate model studies that quantify the impacts of tides and surface waves on convective precipitation and MJO in the maritime continent.

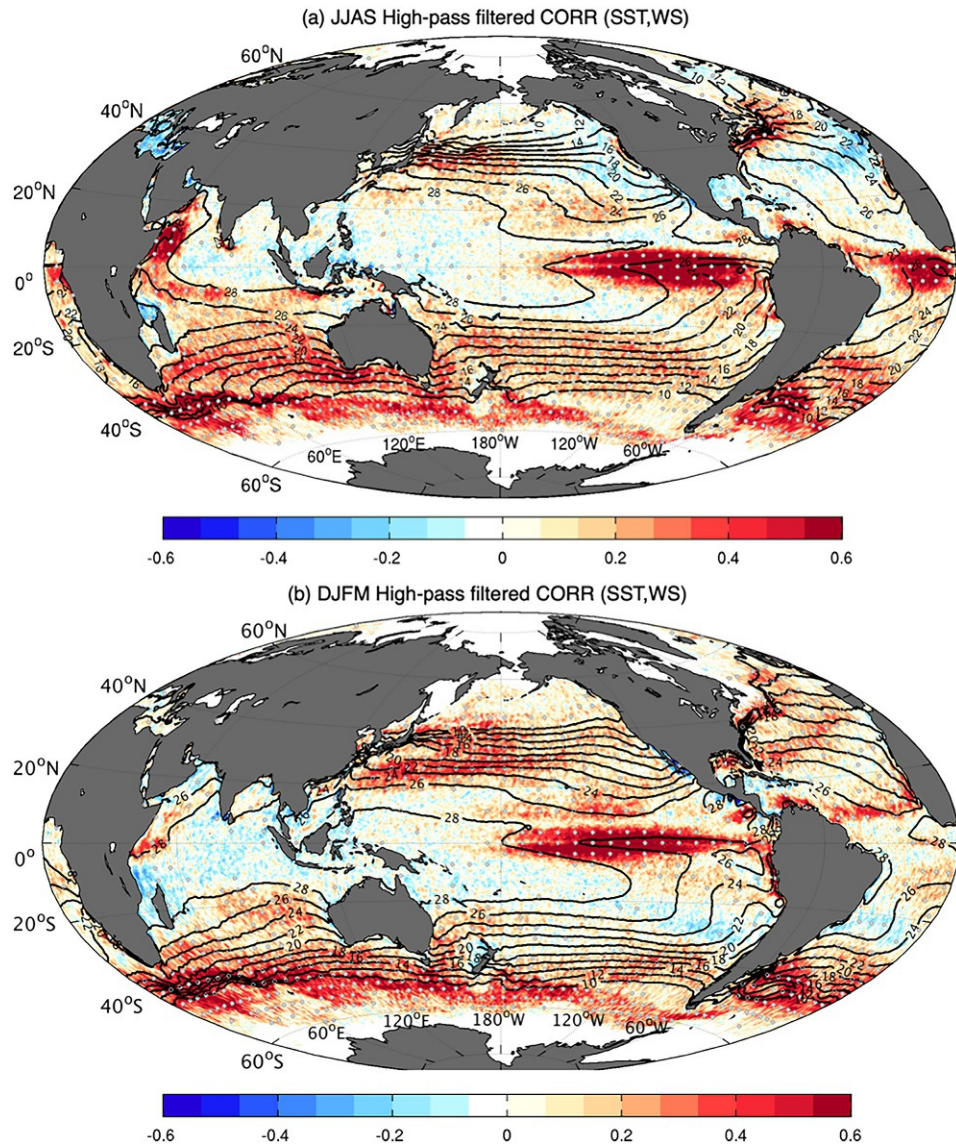


**FIG. 3** Maps of correlation coefficients between daily NOAA-OI SST and surface wind speed from QuikSCAT for (a) boreal summer (June–September) and (b) boreal winter (December–March) of 2001–2009. Wind speed and SST are zonally high-pass filtered ( $10^{\circ}$  longitudes) to remove large-scale air-sea coupling. The black contours denote the climatological SST [ $CI = 2^{\circ}\text{C}$ ] and the gray dots denote the significant correlation at the 95% level. The correlation is positive over most global oceans, including the western Indian Ocean in boreal summer and the southern Indian Ocean year around, indicating that rich mesoscale SST variability there induces local responses in wind speed. (Adapted from Seo (2017).)

#### 4.1.4 Upper-ocean processes

Other processes well-suited for regional coupled climate model studies include the air-sea interaction associated with better resolved upper ocean processes, including the barrier layer and the diurnal SST variability. Here, examples of some of these processes are briefly summarized.

Shenoi et al. (2002) hypothesized that positive feedback exists over the Bay of Bengal during the Indian summer monsoon. The thick barrier layer forced by strong freshwater forcing suppresses the vertical mixing and increases the SST. This leads to enhanced Indian summer monsoon rainfall and higher river discharges, in turn reinforcing the thick barrier layer. Seo et al. (2009) used a 25-km regional coupled climate model to explore the SST and precipitation responses to the enhanced stratification in the Bay of Bengal. Their results support this positive feedback, but the identified SST and precipitation responses were generally weak and limited geographically near the major river mouths. However, their model significantly underestimated the observed upper-ocean stratification in the Bay of Bengal with cold SST bias, and hence it

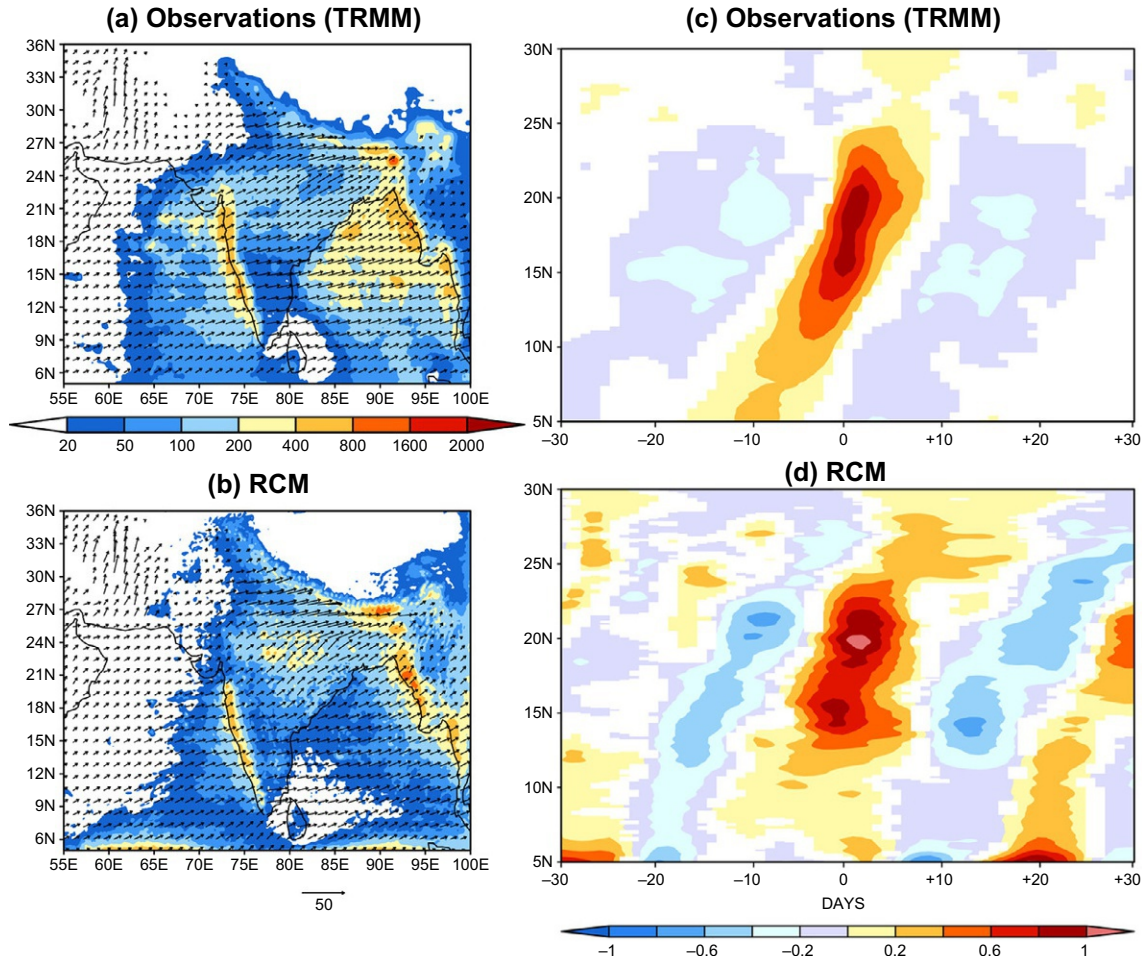


**FIG. 4** (Left) ISV (20–90 days) variances of rainfall (shaded;  $\text{mm}^2/\text{day}^2$ ) and 850-hPa winds (vectors;  $\text{m}^2/\text{s}^2$ ) from (a) TRMM (Tropical Rainfall Measuring Mission) and (b) a regional coupled climate model. The vectors represent the variance of the zonal and meridional wind components. (Right) The regression of zonally averaged ISV rainfall between 70 and 95°E on the ISV rainfall anomalies over central India (75–85°E and 15–25°N) from (c) TRMM and (d) a regional coupled climate model. Negative (positive) lags denote that central Indian rainfall anomalies lead (lag) to the zonally averaged rainfall anomaly. (Adapted from Misra et al. (2018).)

remains unclear if and how such mean state biases affect the sensitivity of the Indian summer monsoon rainfall responses. Krishnamohan et al. (2019) revisited this problem using the 25-km regional coupled climate model of Samson et al. (2014) and explained that the weak SST response results from two compensating effects; while the barrier layer suppresses the vertical mixing and increases the mixed layer temperature, the associated temperature increase is quickly damped by turbulent heat flux via air-sea interaction, leaving only a small net change in SST.

Until recently, conventional CMIP-class global climate models did not consider subdaily air-sea interaction due to increased computational burdens associated with frequent model coupling and/or lack of relevant physics for subdaily air-sea coupling and turbulent vertical mixing. Yet, the importance of the SST diurnal cycle in the tropical oceans has long been recognized (Soloviev & Lukas, 1996; Weller & Anderson, 1996), especially in the context of modulation of ISV (Ruppert & Johnson, 2015; Shinoda, 2005; Shinoda et al., 2021; Sui et al., 1997). Seo et al. (2014) examined the impacts of resolving diurnal SSTs in simulations of the MJO, where the diurnal coupling effect is adjusted by varying the coupling frequency between 1 and 24 h. The resolved diurnal variability with higher coupling frequency (1 h) during the suppressed MJO phase raises the time-mean SST and moistens the low-troposphere, facilitating the subsequent convection. Zhao and Nasuno (2020) used the 7 km regional coupled climate model of Warner et al. (2010) with varied coupling frequency to quantify the impact of subdaily air-sea interaction over the maritime continent. They suggest that the higher model coupling frequency (1 h or shorter) leads to the warmer pre-convection SST aided by shallower mixed layer depth, leading to the more vigorous MJO convection.

## 4.2 Synthesis, issues, and outlook

Recent regional coupled climate model studies in the Indian Ocean have demonstrated significant “added values” in the context of advancing process-level understanding of air-sea interaction and upper ocean processes and their large-scale impacts. However, several challenges remain, many of which are not unique to the regional coupled climate model or the Indian Ocean, as reviewed previously (Schrum, 2017; Xue et al., 2020). But some of these generic issues can be amplified by the regional coupled climate models. One such example is the their inability to represent a realistic ocean mean state in some areas of the Indian Ocean. In regional coupled climate models, additional internal variability arises from better-resolved air-sea interaction, such that slight mean state bias can be amplified by the air-sea coupling. This is in contrast to uncoupled regional models where the observed states are prescribed as surface forcing.

The most striking ocean mean state bias may be found in the northern Indian Ocean during the Indian summer monsoon (e.g., Goswami et al., 2016), especially in the Bay of Bengal, where existing regional coupled climate models exhibit significant cold bias (Krishnamohan et al., 2019; Misra et al., 2018; Seo et al., 2009, 2019). The thermal coupling of the boreal summer intraseasonal oscillation with the oceans is likely to be influenced by the cold bias of SST, which otherwise would hover above the convective thresholds and support the moist convection. The parameterized turbulent mixing schemes in the ocean tend to overestimate the mixing given the wind stress in the BoB, failing to maintain the observed salinity-driven stratification (e.g., Goswami et al., 2016). The coastal upwelling along India’s east coast also tends to be strong in high-resolution regional coupled climate models, providing for the cold bias in the interior basin. Such basin-scale bias persists even with strong salinity restoring (Seo et al., 2019), realistic wind stress forcings (Krishnamohan et al., 2019), or at exceptionally high-model resolutions (Seo et al., 2019). Recent field experiments in the Bay of Bengal (e.g., Vinayachandran et al., 2018; Wijesekara et al., 2016) revealed the intricate patterns of upper-ocean variability and vertical fluxes driven by fine-scale ocean dynamics, leading to the formation of interleaving layers and submesoscale restratification (e.g., Jaeger et al., 2020; Ramachandran et al., 2018). These observed phenomena are not well parameterized in the current ocean models (Chowdary et al., 2016). The excessive vertical mixing and the cooler SST bias are reinforced by the too strong wind bias typical of high-resolution atmospheric modeling.

Other notable regions of significant ocean mean state biases can be found in the Arabian Sea (Weller et al., 2002), where wind-driven mixing and ocean mesoscale dynamics dominate the mixed layer temperature balance, and the maritime continent, where vertical mixing due to tides and the diurnal cycle rectify the ocean mean state and atmosphere-ocean coupling. These regions deserve further regional coupled climate model studies with special attention to the physical representation of upper ocean physics and oceanic mesoscale processes. These include, but are not limited to, vertical mixing affected by the symmetric instability (Bachman & Taylor, 2014; Dong et al., 2021), Langmuir turbulence (Kantha & Clayson, 2004; Li et al., 2016), diurnal cycle (Danabasoglu et al., 2006; Takaya et al., 2010), and wave impacts on ocean mixing and wind stress (Pianezze et al., 2018; Shi & Bourassa, 2019), and mesoscale eddy impacts on air-sea heat fluxes (Bishop et al., 2020).

## 5 Biogeochemistry

### 5.1 Modeling phytoplankton bloom dynamics in the Indian Ocean

#### 5.1.1 Arabian Sea

The Arabian Sea is an exceptionally unique and productive marine ecosystem. Summer monsoon southwesterly winds drive upwelling along the coasts of Oman and Somalia, whereas winter northeasterly winds cause convective mixing in its northern part; each bringing nutrients from the deep into the well-lit upper ocean, driving two major phytoplankton blooms per year (Wiggert et al., 2005). Early coupled physical-biogeochemical modeling efforts of the Arabian Sea have focused on the study of phytoplankton bloom dynamics and its seasonal variability (Hood et al., 2003; McCreary et al., 1996; Ryabchenko et al., 1998). Using intermediate complexity physical models coupled to simple nutrient-phytoplankton-zooplankton-detritus ecosystem models, these pioneering works highlighted the critical role of wind-driven mixing in the bloom dynamics and identified distinct physical processes such as upwelling, entrainment, and detrainment that control Arabian Sea phytoplankton blooms. Despite relative success in reproducing several observed bloom characteristics, these models showed some fundamental flaws associated with deficiencies in the representation of circulation in the Arabian Sea region (Friedrichs et al., 2006; Hood et al., 2003). Many of these discrepancies may be traceable to the inaccurate climatological forcing employed in these studies as well as the inaccurate representation of mixed layer and lateral export of nutrients associated with eddies and filaments in coarse resolution models (Hood et al., 2003; Wiggert et al., 2005, 2006). Indeed, mesoscale and submesoscale eddies and filaments have been suggested to play a dominant role

in advecting nutrients from the coastal upwelling region into the central and northern Arabian Sea (e.g., Koné et al., 2009). Using an eddy-resolving ( $1/12^\circ$ ) horizontal resolution model of the northern Indian Ocean, Resplandy et al. (2011) found that mesoscale eddies substantially increase nutrient supply to the surface and the oligotrophic open sea through both vertical eddy-mixing and lateral stirring. This in turn results in enhanced biological productivity and an improved agreement of the model with observations relative to coarse resolution models.

While modeling studies suggest that nitrogen is generally the most limiting nutrient of biological productivity in the Arabian Sea, silicate and iron have also been suggested to limit productivity locally and intermittently (see also Hood et al., 2024a). For instance, Koné et al. (2009) have shown that silicate limitation becomes dominant in local patches along the west coast of India. In another modeling study of the northern Indian Ocean, Resplandy et al. (2011) found that silicate limitation can also be important in the northern Arabian Sea during the northeast monsoon season. Finally, while the modeling studies of Koné et al. (2009) and Resplandy et al. (2011) suggest that iron limitation is rather marginal in the Arabian Sea, previous works by Wiggert et al. (2006) and Wiggert and Murtugudde (2007) indicate that the region off the coasts of Somalia and Oman is prone to iron limitation during both summer and winter monsoon seasons (see also Hood et al., 2024a). A recent modeling study by Guieu et al. (2019) confirms the critical role that iron input through dust deposition plays in fueling biological production in the Arabian Sea. Indeed, this study suggests that nearly half of summer primary production in the Arabian Sea is dependent on iron supply through eolian dust deposition (Fig. 5).

### 5.1.2 Bay of Bengal

Biological productivity in the Bay of Bengal is weaker than in the Arabian Sea, especially during the summer monsoon season (Prasanna Kumar et al., 2002) despite the presence of coastal upwelling in the northwestern area driven by the Fidjilater jet during the summer monsoon season (Gomes et al., 2000; Lévy et al., 2007). This is thought to be caused by the large freshwater input through rivers and rainfall that leads to the formation of a barrier layer near the surface limiting vertical mixing and nutrient transfer from the subsurface (e.g., Gomes et al., 2000; Vinayachandran et al., 2002b). Previous modeling work suggests that the bloom in the northwestern sector is essentially driven by upwelling and vertical mixing (Koné et al., 2009). During the northeast monsoon, observations reveal higher surface chlorophyll concentrations in the

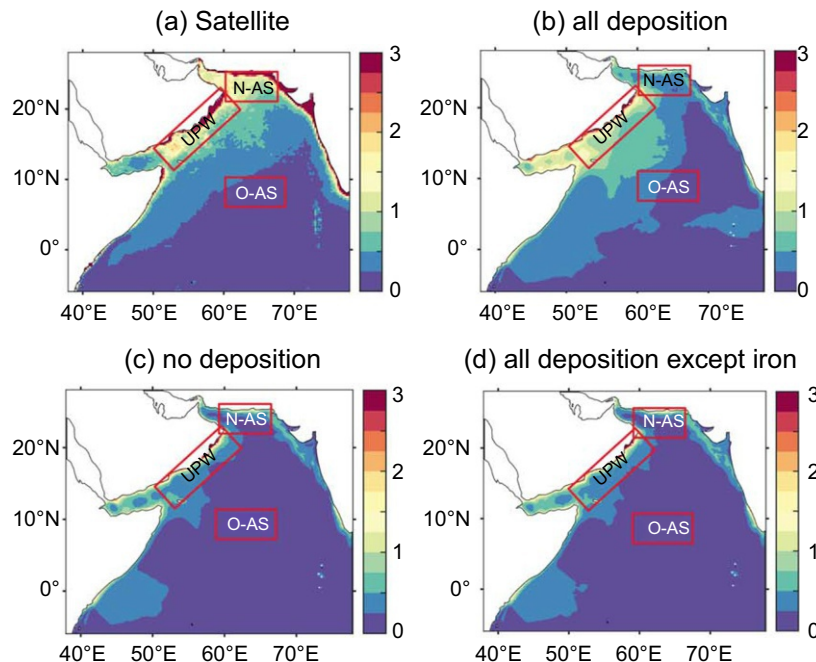


**FIG. 5** Impact of nutrient atmospheric deposition on Arabian Sea productivity. Annual patterns of Chl-a ( $\text{mg m}^{-3}$ ) in satellite data (a) and model simulation with (b) atmospheric deposition of soluble iron, nitrogen, and phosphate (all deposition), (c) no atmospheric deposition of nutrients (zero deposition), and (d) atmospheric deposition of nitrogen and phosphate only (all deposition except iron). Note that the “no deposition” and the “all deposition except iron” simulations fail to properly reproduce the observed Chl-a patterns, in contrast to the simulation where the deposition of all nutrients is taken into account. (Adapted from Guieu et al. (2019).)

western and northwestern Bay of Bengal (Gomes et al., 2000). The dynamics of the phytoplankton bloom during winter in the Bay of Bengal was first investigated using an intermediate complexity coupled physical-biogeochemical model by Vinayachandran et al. (2005). The model was similar to the one used to study the dynamics of blooms in the Arabian Sea by McCreary et al. (1996) and Hood et al. (2003). The model reproduces several characteristics of the observed bloom from the remotely sensed data. Their main finding was that the entrainment of not only subsurface nutrients but also phytoplankton contributes to the observed surface bloom. This entrainment is driven by both Ekman pumping and the deepening of the mixed layer (Vinayachandran et al., 2005). Finally, previous modeling studies suggest that nitrogen is generally the most limiting nutrient during bloom onset in most of the Bay of Bengal, except in limited areas along the east coast of India and in the eastern part of the bay where diatom growth tends to be silicate limited (Koné et al., 2009).

### 5.1.3 Southern tropical Indian Ocean

In the southern tropical Indian Ocean, observations and model simulations reveal the presence of a single bloom peaking in summer (Koné et al., 2009). Due to an upwelling-favorable wind stress curl, the nutricline is relatively shallow between 10°S and 15°S during the summer season. Episodic strong wind events leading to convective mixing cause a deepening of the mixed layer and entrainment of nutrients to the surface there (Koné et al., 2009). Resplandy et al. (2009) explored the biogeochemical response to variability in atmospheric forcing at intraseasonal scales such as that associated with the MJO in the SCTR. Using a coupled physical-biogeochemical eddy-permitting model of the Indian Ocean, they found that vertical mixing associated with MJO events fertilizes the mixed layer through entrainment, thus enhancing surface biological productivity. They also found that this response is highly sensitive to interannual variability of thermocline depth in the SCTR region.

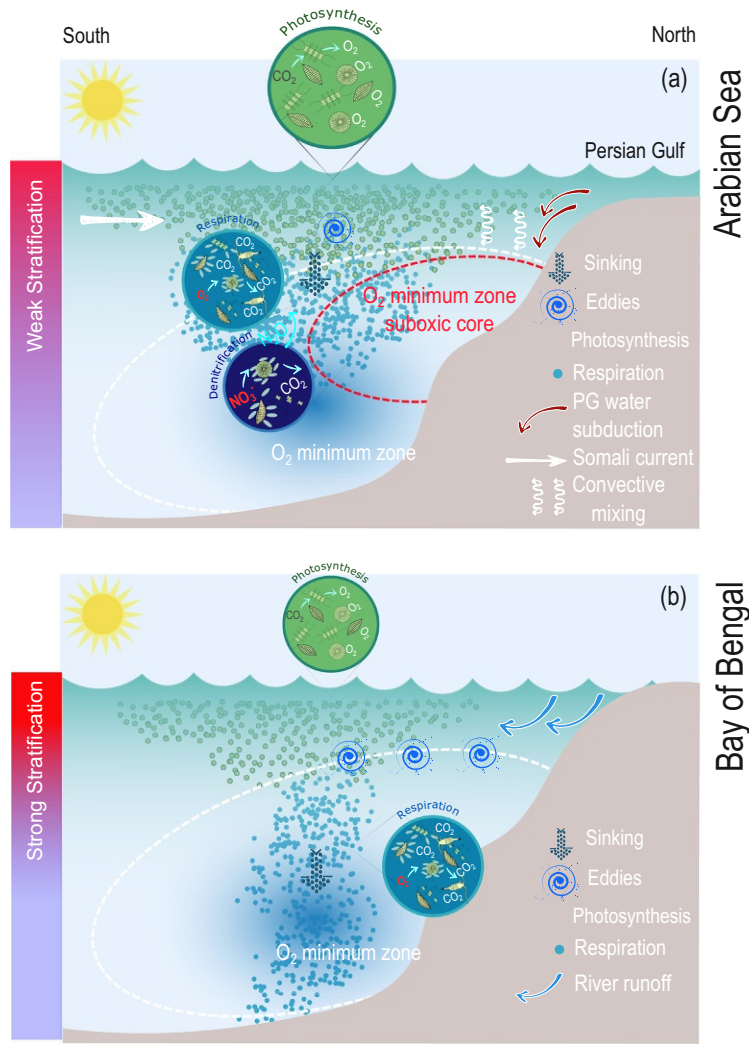
## 5.2 Modeling Indian Ocean oxygen minimum zones (OMZs)

The OMZs of the Arabian Sea and the Bay of Bengal are among the most intense in the world ocean (Hood et al., 2024b; Paulmier & Ruiz-Pino, 2009). While both OMZs display low oxygen concentrations, important contrasts in their intensity are observed. While active denitrification and oxygen levels in the suboxic range ( $< 5 \text{ mmol m}^{-3}$ ) are observed over large swaths of the Arabian Sea, oxygen concentrations in the Bay of Bengal remain above the suboxic thresholds, preventing large-scale denitrification from occurring (Bristow et al., 2017; Hood et al., 2024b). Using a series of model simulations, Al Azhar et al. (2017) have demonstrated that deeper remineralization in the Bay of Bengal driven by faster particle sinking speeds contributes to weakening the OMZ there (see also Hood et al., 2024b). Indeed, ballast minerals associated with the large riverine input in the Bay of Bengal increase the particle sinking speed, thus reducing the organic matter residence time in the OMZ layer, and hence weakening the oxygen consumption there. Additional factors have been identified as potentially contributing to the varying OMZ intensity between the two seas (Fig. 6). For instance, McCreary et al. (2013) investigated the role of lateral advection and transport of organic matter in controlling the oxygen distribution in the Arabian Sea and Bay of Bengal. Their modeling work highlights the importance of lateral transport of organic matter from the western Arabian Sea into the central and eastern sectors of the Arabian Sea, where it enhances remineralization and contributes to lowering O<sub>2</sub> levels to below suboxic thresholds. According to these authors, the lack of such a source of organic matter in the Bay of Bengal may contribute to the weakness of its OMZ. In addition, differences in the intensity of eddy activity between the two OMZs have also been suggested to contribute to their contrasting intensities. Indeed, as eddies were shown to dominate both the vertical and lateral supply of oxygen in the Arabian Sea (Lachkar et al., 2016; Resplandy et al., 2012), the higher eddy activity in the Bay of Bengal may contribute to weakening its OMZ intensity (Sarma & Udaya Bhaskar, 2018).

## 5.3 Modeling Indian Ocean ecosystems under a warmer climate

The northern and western tropical Indian Ocean have experienced strong warming throughout most of the twentieth century, accelerating since the early 1990s (Kumar et al., 2009; Roxy et al., 2014, 2024). This warming has the potential to alter the marine ecosystems and the biogeochemistry of the region. For instance, using satellite observations as well as hindcast simulations, Roxy et al. (2016) found a significant drop in biological productivity in the western Indian Ocean that they attributed to enhanced vertical stratification suppressing vertical mixing and limiting nutrient supply from the ocean interior to the surface (see also Hood et al., 2024a). Their analysis has also suggested that the projected future warming in the region will likely cause a further decline in its biological productivity. Recent model projections confirm a general future decline of summer productivity in the western Indian Ocean and the Arabian Sea with important implications for the biological pump of carbon and fisheries (Bindoff et al., 2019; Kwiatkowski et al., 2020). In addition to increased stratification and dropping productivity, the ongoing surface warming in the northern and western Indian Ocean is also predicted to

**FIG. 6** The contrasts in oxygen minimum zone (OMZ) intensity between the Arabian Sea and the Bay of Bengal and their potential drivers. (a) Despite stronger ventilation from the south (Somali Current) and in the north (associated with Persian Gulf water subduction and winter convective mixing), a very large flux of organic matter remineralized at shallow depth in the Arabian Sea leads to an intense OMZ with an important shallow denitrifying suboxic core. (b) A stronger stratification, a deeper remineralization due to ballasting by riverine particles, and stronger ventilation by eddies limit the intensity of the OMZ and prevent the occurrence of large-scale denitrification.



affect the Indian Ocean OMZs (Kwiatkowski et al., 2020). Yet, these projections come with high uncertainties that stem from multiple factors among which the representation of mixing in earth system models (Lévy et al., 2021), the strong sensitivity of OMZs to subtle changes in the balance between ventilation-driven O<sub>2</sub> replenishment and biology-induced O<sub>2</sub> depletion (Resplandy, 2018), and the uncertainty around future regional changes in Indian monsoon winds (e.g., Lachkar et al., 2018).

## 6 Conclusions and discussion

Ocean circulation and upper-ocean structure over the Indian Ocean are unique and complex. For example, a large seasonal cycle of upper-ocean currents is found almost everywhere in the tropics such as the seasonal reversal of low-latitude western boundary currents due to the strong influence of the monsoon on the ocean. Because of the improvement of large-scale high-resolution ocean GCMs in recent years, the mean and seasonal cycle of major ocean currents and upper-ocean structure, including narrow boundary currents, are now simulated by ocean models reasonably well. Yet quantitative comparisons with observations are still difficult in many locations because of the sparse coverage of in situ measurements. While recent satellite observations can be used to estimate surface current variability, it is still difficult to characterize the detailed structure of narrow boundary currents. Also, subsurface data are necessary to estimate the transport of major currents. Although the coverage of in situ measurements has been substantially improved in recent years due to Argo float measurements since the early 2000s (McPhaden et al., 2024; Phillips et al., 2024), it may not be sufficient for the comprehensive evaluation of model performance on different time scales in many locations such as the interior southern Indian Ocean.

Ocean GCMs' ability to reproduce SSTs over the Indian Ocean is crucial for climate model simulation and prediction, and comparisons with satellite-derived SSTs suggest that many models can simulate the mean and seasonal cycle of SST

reasonably well. However, there are still a number of issues for evaluating the model performance quantitatively. For example, SST simulations of ocean GCMs critically depend on the quality of surface fluxes of heat, momentum, and freshwater. Yet a significant uncertainty exists in these surface fluxes (e.g., Yu, 2019), and thus model errors in SSTs are partly due to the errors in surface fluxes. The uncertainty of surface fluxes, especially surface heat fluxes, needs to be reduced for further quantitative evaluation of the model performance.

Upper ocean salinity stratification is shown to be important to control SSTs in the tropical Indian Ocean. In particular, accurate simulations of strong salinity stratification and thick barriers in the Bay of Bengal may largely influence SSTs. However, evaluating a model's capability of simulating sea surface salinity and subsurface salinity stratification is still challenging because of the uncertainty of surface freshwater fluxes and river runoff. Significant errors in the upper ocean salinity over the Bay of Bengal are evident in most ocean GCMs. These errors are partly caused by the uncertainty of freshwater input and model deficiencies, such as mixing parameterization, and the relative magnitude of these errors is still unknown.

Model simulation and prediction of climate variability over the Indian Ocean (such as IOD) using coupled ocean-atmosphere models have been improving in recent years. Some IOD events have been predicted with a lead time of one or two seasons, but the prediction skill is often reduced due to various prediction challenges such as the winter prediction barrier (Yamagata et al., 2024). To further improve current climate model simulations, it is at least necessary to advance our understanding of oceanic, atmospheric, and regional air-sea coupled processes associated with climate variability not only over the Indian Ocean but also in other ocean basins. For example, IOD is influenced by climate variability in other ocean basins including ENSO in the Pacific. Hence, simulation and prediction of Indian Ocean climate variability critically depend on simulations in other regions including ENSO in the Pacific. Dynamical and physical processes for the generation and development of climate variability such as IOD and Ningaloo Niño are not well understood (see also Yamagata et al., 2024). A better understanding of interbasin interaction of climate variability may help to improve climate prediction in the Indian Ocean by climate models.

Since biogeochemical processes are largely influenced by physical processes such as ocean currents, upwelling/downwelling, mixing, and upper ocean temperature changes, coupled biological/physical models that include adequate representations of physical processes are necessary to examine the unique biogeochemical processes in the Indian Ocean. Biogeochemical modeling in the Indian Ocean has become an active research area in recent years. For example, simulating the generation and maintenance of large OMZs in the Arabian Sea is one of the focus areas in recent research efforts. Identifying significant changes in the ecosystem in the Indian Ocean under a warming climate using coupled biological/physical modeling and observations has also been a focus of recent studies.

## 7 Educational resources

The source codes of some of the state-of-the-art ocean models, atmospheric models, and coupled models are publicly available. For example, major OGCMs widely used in climate research are mostly community models. Web sites of these community models are listed in the following:

### Ocean GCMs

- Modular Ocean Model version 6 (MOM6). <https://github.com/NOAA-GFDL/MOM6-examples/wiki>
- Hybrid Coordinate Ocean Model (HYCOM). <https://www.hycom.org>
- Regional Ocean Modeling System (ROMS). <https://www.myroms.org>
- MITgcm. <http://mitgcm.org>

### Atmosphere GCMs

- The Community Atmosphere Model. <http://www.cesm.ucar.edu/models/cesm2/atmosphere/>
- FV3GFS (Finite Volume 3 Global Forecast System). <https://github.com/NOAA-EMC/fv3gfs>

### Coupled Atmosphere-Ocean GCMs

- Community Earth System Model. <http://www.cesm.ucar.edu>
- Unified Forecast System (UFS). <https://ufscommunity.org>

### Regional coupled model

- Scripps Coupled Ocean-Atmosphere Regional (SCOAR) Model. <https://github.com/hyodae-seo/SCOAR>

## Acknowledgments

TS acknowledges support from National Oceanic and Atmospheric Administration Grant NA17OAR4310256 and DOD Grant W911NF-20-1-0309. TGJ is sponsored by the U.S. Office of Naval Directed Research Initiative PISTON (73-4347-27-5). HS is grateful for support from National Oceanic and Atmospheric Administration NA17OAR4310255 and ONR N00014-17-1-2398. ZL is supported by Tamkeen through Research Institute grant CG009 to the NYUAD Arabian Center for Climate and Environmental Sciences (ACCESS). YM is supported by the Japan Society for the Promotion of Science KAKENHI Grant Number JP17H01663.

## Author contributions

TS led the overall writing, editing and organization of the manuscript. TS wrote [Sections 1 and 6](#); TGJ and TS wrote [Section 2](#); YM wrote [Section 3](#); HS wrote [Section 4](#); ZL wrote [Section 5](#); all authors wrote [Section 7](#). All authors contributed comments and feedback on overall structure of the chapter and contributed to revisions.

## References

- Al Azhar, M., Lachkar, Z., Lévy, M., & Smith, S. (2017). Oxygen minimum zone contrasts between the Arabian Sea and the Bay of Bengal implied by differences in remineralization depth. *Geophysical Research Letters*, 44(21), 11–106.
- Aldrian, E., Sein, D., Jacob, D., Gates, L. D., & Podzun, R. (2005). Modelling Indonesian rainfall with a coupled regional model. *Climate Dynamics*, 25(1), 1–17.
- Anderson, D. L. T., & Carrington, D. (1993). Modeling interannual variability in the Indian Ocean using momentum fluxes from the operational weather analyses of the United Kingdom Meteorological Office and European Centre for Medium Range Weather Forecasts. *Journal of Geophysical Research*, 98, 12483–12499.
- Anderson, D. L. T., & Moore, D. W. (1979). Cross-equatorial inertial jets with special relevance to very remote forcing of the Somali current. *Deep Sea Research*, 26, 1–22.
- Bachman, S. D., & Taylor, J. R. (2014). Modeling of partially-resolved oceanic symmetric instability. *Ocean Modelling*, 82, 15–27.
- Beal, L. M., & Bryden, H. L. (1999). The velocity and vorticity structure of the Agulhas Current at 32°S. *Journal of Geophysical Research*, 104(C3), 5151–5176.
- Beal, L. M., Chereskin, T. K., Bryden, H. L., & Ffield, A. (2003). Variability of water properties, heat and salt fluxes in the Arabian Sea, between the onset and wane of the 1995 Southwest monsoon. *Deep Sea Research, Part II*, 50, 2049–2075.
- Beal, L. M., & Donohue, K. A. (2013). The Great Whirl: Observations of its seasonal development and interannual variability. *Journal of Geophysical Research-Oceans*, 118, 1–13. <https://doi.org/10.1029/2012JC008198>.
- Beal, L. M., Eliot, S., Houk, A., & Leber, G. M. (2015). Capturing the transport variability of a western boundary jet: Results from the Agulhas Current Time-Series Experiment (ACT). *Journal of Physical Oceanography*, 45, 1302–1324. <https://doi.org/10.1175/JPO-D-14-0119.1>.
- Beal, L., et al. (2020). A roadmap to IndOOS-2: Better observations of the rapidly-warming Indian Ocean. *Bulletin of the American Meteorological Society*, 1–50.
- Biastoch, A., Sein, D., Durgadoo, J. V., Wang, Q., & Danilov, S. (2018). Simulating the Agulhas system in global ocean models—Nesting vs. multi-resolution unstructured meshes. *Ocean Modelling*, 121(2018), 117–131. <https://doi.org/10.1016/j.ocemod.2017.12.002>.
- Bindoff, N. L., Cheung, W. W., Kairo, J. G., Arístegui, J., Guinder, V. A., Hallberg, R., ... Williamson, P. (2019). *Changing ocean, marine ecosystems, and dependent communities. IPCC special report on the ocean and cryosphere in a changing climate* (pp. 477–587).
- Bishop, S. P., Small, R. J., & Bryan, F. O. (2020). The global sink of available potential energy by mesoscale air-sea interaction. *Journal of Advances in Modeling Earth Systems*, 12, e2020MS002118.
- Bristow, L. A., Callbeck, C. M., Larsen, M., Altabet, M. A., Dekaezemacker, J., Forth, M., & Canfield, D. E. (2017). N2 production rates limited by nitrite availability in the bay of Bengal oxygen minimum zone. *Nature Geoscience*, 10(1), 24–29.
- Bruce, J. (1973). Equatorial undercurrent in the western Indian Ocean during the southwest monsoon. *Journal of Geophysical Research*, 78, 6386–6394. <https://doi.org/10.1029/JC078i027p06386>.
- Bryden, H. L., Beal, L. M., & Duncan, L. (2005). Structure and transport of the Agulhas current and its temporal variability. *Journal of Oceanography*, 61, 479–492. <https://doi.org/10.1007/s10872-005-0057-8>.
- Cane, M., & Moore, D. W. (1981). A note on low-frequency equatorial basin modes. *Journal of Physical Oceanography*, 11, 1578–1584.
- Chelton, D. B., Schlax, M. G., Samelson, R. M., & de Szoeke, R. A. (2007). Global observations of large oceanic eddies. *Geophysical Research Letters*, 34 (L15606). <https://doi.org/10.1029/2007GL030812>.
- Chen, S., Campbell, T. J., Jin, H., Gabersek, S., Hodur, R. M., & Martin, P. (2010). Effect of two-way air-sea coupling in high and low wind speed regimes. *Monthly Weather Review*, 138, 3579–3602.
- Chen, G. X., Han, W. Q., Li, Y. L., Yao, J., & Wang, D. (2019a). Intraseasonal variability of the equatorial undercurrent in the Indian Ocean. *Journal of Physical Oceanography*, 45, 85–101.
- Chen, G. X., Han, W. Q., Li, Y. L., Wang, D. X., & McPhaden, M. J. (2019b). Seasonal-to-interannual time-scale dynamics of the equatorial undercurrent in the Indian Ocean. *Journal of Physical Oceanography*, 45, 1532–1553.
- Chowdary, J. S., Srinivas, G., Fousiya, T. S., Parekh, A., Gnanaseelan, C., Seo, H., & MacKinnon, J. A. (2016). Representation of Bay of Bengal upper-ocean salinity in general circulation models. *Oceanography*, 29(2), 38–49. <https://doi.org/10.5670/oceanog.2016.37>.

- Church, J. A., Cresswell, G. R., & Godfrey, J. S. (1989). The Leeuwin current. In S. J. Neshyba, C. N. K. Moors, R. L. Smith, & R. T. Barber (Eds.), *34. Polewardflows along eastern ocean boundaries. Coastal and estuarine studies* (pp. 230–254). New York: Springer.
- Cox, M. D. (1970). A mathematical model of the Indian Ocean. *Deep Sea Research*, *17*, 47–75.
- Cox, M. D. (1976). Equatorially trapped waves and the generation of the Somali Current. *Deep Sea Research*, *23*, 1139–1152.
- Cresswell, G. R., & Golding, T. J. (1980). Observations of a south-flowing current in the southeastern Indian Ocean. *Deep Sea Research*, *27*, 449–466.
- Danabasoglu, G., Large, W. G., Tribbia, J. J., Gent, P. R., Briegleb, B. P., & McWilliams, J. C. (2006). Diurnal coupling in the tropical oceans of CCSM3. *Journal of Climate*, *19*(11), 2347–2365.
- Delman, A. S., McClean, J. L., Sprintall, J., Talley, L. D., & Bryan, F. O. (2018). Process-specific contributions to anomalous Java mixed layer cooling during positive IOD events. *Journal of Geophysical Research: Oceans*, *123*, 4153–4176. <https://doi.org/10.1029/2017JC013749>.
- DeMott, C. A., Klingaman, N. P., & Woolnough, S. J. (2015). Atmosphere-ocean coupled processes in the Madden-Julian oscillation. *Reviews of Geophysics*, *53*, 1099–1154. <https://doi.org/10.1002/2014RG000478>.
- DeMott, C. A., Ruppert, J. H., Jr., & Rydbeck, A. (2024). Chapter 4: Intraseasonal variability in the Indian Ocean region. In C. C. Ummenhofer, & R. R. Hood (Eds.), *The Indian Ocean and its role in the global climate system* (pp. 79–101). Amsterdam: Elsevier. <https://doi.org/10.1016/B978-0-12-822698-8.00006-8>.
- DeMott, C. A., Stan, C., & Randall, D. A. (2013). Northward propagation mechanisms of the boreal summer intraseasonal oscillation in the ERA-Interim and SP-CCSM. *Journal of Climate*, *26*, 1973–1992.
- Doi, T., Behera, S. K., & Yamagata, T. (2016). Improved seasonal prediction using the SINTEX-F2 coupled model. *Journal of Advances in Modeling Earth Systems*, *8*(4), 1847–1867. <https://doi.org/10.1002/2016MS000744>.
- Doi, T., Behera, S. K., & Yamagata, T. (2019). Merits of a 108-member ensemble system in ENSO and IOD predictions. *Journal of Climate*, *32*, 957–972.
- Doi, T., Behera, S. K., & Yamagata, T. (2020). Predictability of the super IOD event in 2019 and its link with El Niño Modoki. *Geophysical Research Letters*, *47*. <https://doi.org/10.1029/2019GL086713>.
- Doi, T., Storto, A., Behera, S. K., Navarra, A., & Yamagata, T. (2017). Improved prediction of the Indian Ocean dipole mode by use of subsurface ocean observations. *Journal of Climate*, *30*, 7953–7970. <https://doi.org/10.1175/JCLI-D-16-0915.1>.
- Dong, J., Fox-Kemper, B., Zhu, J., & Dong, C. (2021). Application of symmetric instability parameterization in the coastal and Regional Ocean community model (CROCO). *Journal of Advances in Modeling Earth Systems*, *13*.
- Duvel, J. P., Roca, R., & Vialard, J. (2004). Ocean mixed layer temperature variations induced by intraseasonal convective perturbations over the Indian Ocean. *Journal of the Atmospheric Sciences*, *61*, 1004–1022.
- Effy, J. B., Francis, P. A., Ramakrishna, S. S. V. S., & Mukherjee, A. (2020). Anomalous warming of the western equatorial Indian Ocean in 2007: Role of ocean dynamics. *Ocean Modelling*, *147*, 101542. <https://doi.org/10.1016/j.ocemod.2019.101542>.
- Feng, R., & Duan, W. S. (2019). Indian Ocean Dipole-related predictability barriers induced by initial errors in the tropical Indian Ocean in a CGCM. *Advances in Atmospheric Sciences*, *36*(6), 658–668. <https://doi.org/10.1007/s00376-019-8224-9>.
- Feng, R., Duan, W., & Mu, M. (2014). The “winter predictability barrier” for IOD events and its error growth dynamics: Results from a fully coupled GCM. *Journal of Geophysical Research, Oceans*, *119*, 8688–8708. <https://doi.org/10.1002/2014JC010473>.
- Feng, M., Lengaigne, M., Manneula, S., Gupta, A. S., & Vialard, J. (2024). Chapter 6: Extreme events in the Indian Ocean: Marine heatwaves, cyclones, and tsunamis. In C. C. Ummenhofer, & R. R. Hood (Eds.), *The Indian Ocean and its role in the global climate system* (pp. 121–144). Amsterdam: Elsevier. <https://doi.org/10.1016/B978-0-12-822698-8.00011-1>.
- Feng, M., McPhaden, M. J., Xie, S.-P., & Hafner, J. (2013). La Niña forces unprecedented Leeuwin Current warming in 2011. *Scientific Reports*, *3*, 1–9. <https://doi.org/10.1038/srep01277>.
- Feng, X., Shinoda, T., & Han, W. (2023). Topographic trapping of the Leeuwin Current and its impact on the 2010/11 Ningaloo Niño. *Journal of Climate*, *36*(6), 1587–1603. <https://doi.org/10.1175/JCLI-D-22-0218.1>.
- Fischer, A. S., Terray, P., Guilyardi, E., Gualdi, S., & Delecluse, P. (2004). Two independent triggers for the Indian Ocean dipole/zonal mode in a coupled GCM. *Journal of Climate*, *18*, 3428–3449.
- Friedrichs, M. A., Hood, R. R., & Wiggert, J. D. (2006). Ecosystem model complexity versus physical forcing: Quantification of their relative impact with assimilated Arabian Sea data. *Deep Sea Research Part II: Topical Studies in Oceanography*, *53*(5–7), 576–600.
- Fu, X., Wang, B., Waliser, D. E., & Tao, L. (2007). Impact of atmosphere—Ocean coupling on the predictability of monsoon intraseasonal oscillations. *Journal of the Atmospheric Sciences*, *64*, 157–174.
- Fu, X., Yang, B., Bao, Q., & Wang, B. (2008). Sea surface temperature feedback extends the predictability of tropical intraseasonal oscillation. *Monthly Weather Review*, *136*, 577–597.
- Furue, R. (2019). The three-dimensional structure of the Leeuwin Current System in density coordinates in an eddy-resolving OGCM. *Ocean Modelling*, *138*, 36–50. <https://doi.org/10.1016/j.ocemod.2019.03.001>.
- Gent, P. R. (1981). Forced standing equatorial ocean wave modes. *Journal of Marine Research*, *39*, 695–709.
- Giorgi, F. (2019). Thirty years of regional climate modeling: Where are we and where are we going next? *Journal of Geophysical Research-Atmospheres*, *124*, 5696–5723.
- Godfrey, J. S. (1989). A Sverdrup model of the depth-integrated flow for the world ocean allowing for island circulations. *Geophysical and Astrophysical Fluid Dynamics*, *45*, 89–112. <https://doi.org/10.1080/03091928908208894>.
- Godfrey, J. S., & Weaver, A. J. (1991). Is the Leeuwin Current driven by Pacific heating and winds? *Progress in Oceanography*, *27*, 225–272.
- Gomes, H. R., Goes, J. I., & Saino, T. (2000). Influence of physical processes and freshwater discharge on the seasonality of phytoplankton regime in the Bay of Bengal. *Continental Shelf Research*, *20*(3), 313–330.

- Gordon, A. L. (1985). Indian-Atlantic transfer of thermocline water at the Agulhas retroflection. *Science*, 227, 1030–1033.
- Gordon, A. L., Sprintall, J., Van Aken, H. M., Susanto, D., Wijffels, S., Molcard, R., Ffield, A., Pranowo, W., & Wirasantosa, S. (2010). The Indonesian Throughflow during 2004–2006 as observed by the INSTANT program. *Dynamics of Atmosphere and Oceans*, 50, 115–128. <https://doi.org/10.1016/j.dynatmoce.2009.12.002>.
- Goswami, B. N., Rao, S. A., Sengupta, D., & Chakravorty, S. (2016). Monsoons to mixing in the Bay of Bengal: Multiscale air-sea interactions and monsoon predictability. *Oceanography*, 29(2), 18–27.
- Gualdi, S., Guilyardi, E., Navarra, A., Masina, S., & Delecluse, P. (2003). The interannual variability in the tropical Indian Ocean as simulated by a CGCM. *Climate Dynamics*, 20, 567–582. <https://doi.org/10.1007/s00382-002-0295-z>.
- Guieu, C., Al Azhar, M., Aumont, O., Mahowald, N., Lévy, M., Éthé, C., & Lachkar, Z. (2019). Major impact of dust deposition on the productivity of the Arabian Sea. *Geophysical Research Letters*, 46(12), 6736–6744.
- Halkides, D. J., & Lee, T. (2009). Mechanisms controlling seasonal-to-interannual mixed layer temperature variability in the southeastern tropical Indian Ocean. *Journal of Geophysical Research*, 114, C02012. <https://doi.org/10.1029/2008JC004949>.
- Halkides, D. J., Waliser, D. E., Lee, T., Menemenlis, D., & Guan, B. (2015). Quantifying the processing controlling intraseasonal mixed-layer temperature variability in the tropical Indian Ocean. *Journal of Geophysical Research, Oceans*, 120, 692–715. <https://doi.org/10.1002/2014JC010139>.
- Han, W., McCreary, J. P., Anderson, D. L. T., & Mariano, A. J. (1999). Dynamics of the eastern surface jets in the equatorial Indian Ocean. *Journal of Physical Oceanography*, 29, 2191–2209. [https://doi.org/10.1175/1520-0485\(1999\)029<2191:DOTESJ>2.0.CO;2](https://doi.org/10.1175/1520-0485(1999)029<2191:DOTESJ>2.0.CO;2).
- Han, W., Shinoda, T., Fu, L.-L., & McCreary, J. P. (2006). Impact of atmospheric intraseasonal oscillations on the Indian Ocean dipole during the 1990s. *Journal of Physical Oceanography*, 36, 670–690.
- Han, W., Yuan, D., Liu, W. T., & Halkides, D. J. (2007). Intraseasonal variability of the Indian Ocean Sea surface temperature during boreal winter: Madden-Julian oscillation versus submonthly forcing and processes. *Journal of Geophysical Research*, 112, C04001. <https://doi.org/10.1029/2006JC003791>.
- Hermes, J., & Reason, C. J. C. (2008). Annual cycle of the South Indian Ocean (Seychelles-Chagos) thermocline ridge in a regional ocean model. *Journal of Geophysical Research*, 113, C04035. <https://doi.org/10.1029/2007JC004363>.
- Hadur, R. M. (1997). The naval research Laboratory's coupled ocean/atmosphere mesoscale prediction system (COAMPS). *Monthly Weather Review*, 125, 1414–1430.
- Hood, R. R., Coles, V. J., Huggett, J. A., Landry, M. R., Levy, M., Moffett, J. W., & Rixen, T. (2024a). Chapter 13: Nutrient, phytoplankton, and zooplankton variability in the Indian Ocean. In C. C. Ummenhofer, & R. R. Hood (Eds.), *The Indian Ocean and its role in the global climate system* (pp. 293–327). Amsterdam: Elsevier. <https://doi.org/10.1016/B978-0-12-822698-8.00020-2>.
- Hood, R. R., Kohler, K. E., McCreary, J. P., & Smith, S. L. (2003). A four-dimensional validation of a coupled physical–biological model of the Arabian Sea. *Deep Sea Research Part II: Topical Studies in Oceanography*, 50(22–26), 2917–2945.
- Hood, R. R., Rixen, T., Levy, M., Hansell, D. A., Coles, V. J., & Lachkar, Z. (2024b). Chapter 12: Oxygen, carbon, and pH variability in the Indian Ocean. In C. C. Ummenhofer, & R. R. Hood (Eds.), *The Indian Ocean and its role in the global climate system* (pp. 265–291). Amsterdam: Elsevier. <https://doi.org/10.1016/B978-0-12-822698-8.00017-2>.
- Howden, S. D., & Murtugudde, R. (2001). Effects of river inputs into the Bay of Bengal. *JGR Oceans*, 106, 19825–19843.
- Iizuka, S., Matsuura, T., & Yamagata, T. (2000). The Indian Ocean SST dipole simulated in a coupled general circulation model. *Geophysical Research Letters*, 27, 3369–3372.
- Jaeger, G. S., Lucas, A. J., & Mahadevan, A. (2020). Formation of interleaving layers in the Bay of Bengal. *Deep Sea Research, Part II*, 172, 104717.
- Jayakumar, A., Vialard, J., Lengaigne, M., Gnanaseelan, C., McCreary, J. P., & Kumar, B. P. (2011). Processes controlling the surface temperature signature of the Madden-Julian oscillation in the thermocline ridge of the Indian Ocean. *Climate Dynamics*, 37, 2217–2234.
- Jensen, T. G. (1991). Modeling the seasonal undercurrents in the Somali Current system. *Journal of Geophysical Research-Oceans*, 96, 22151–22167.
- Jensen, T. G. (1993). Equatorial variability and resonance in a wind-driven Indian Ocean model. *Journal of Geophysical Research-Oceans*, 98, 22533–22552.
- Jensen, T. G., Shinoda, T., Chen, S., & Flatau, M. (2015). Ocean response to CINDY/DYNAMO MJOs in air-sea coupled COAMPS. *Journal of the Meteorological Society of Japan*, 93A, 157–178.
- Kantha, L. H., & Clayson, C. A. (2004). On the effect of surface gravity waves on mixing in an oceanic mixed layer model. *Ocean Modelling*, 6, 101–124.
- Karmakar, N., & Misra, V. (2020a). Differences in northward propagation of convection over the Arabian Sea and Bay of Bengal during boreal summer. *Journal of Geophysical Research-Atmospheres*, 125.
- Karmakar, N., & Misra, V. (2020b). The fidelity of a regional coupled model in capturing the relationship between intraseasonal variability and the onset/demise of the Indian summer monsoon. *Climate Dynamics*, 54, 4693–4710.
- Kido, S., Tozuka, T., & Han, W. (2019a). Anatomy of salinity anomalies associated with the positive Indian Ocean Dipole. *Journal of Geophysical Research: Oceans*, 124, 8116–8139. <https://doi.org/10.1029/2019JC015163>.
- Kido, S., Tozuka, T., & Han, W. (2019b). Experimental assessments on impacts of salinity anomalies on the positive Indian Ocean Dipole. *Journal of Geophysical Research: Oceans*, 124, 9462–9486. <https://doi.org/10.1029/2019JC015479>.
- Kindle, J. C., & Thompson, J. D. (1989). The 26- and 50-day oscillations in the Western Indian Ocean: Model results. *Journal of Geophysical Research*, 94, 4721–4736.
- Knauss, J. A., & Taft, B. A. (1964). Equatorial Undercurrent of the Indian Ocean. *Science*, 143, 354–356. <https://doi.org/10.1126/science.143.3604.354>.
- Knox, R. A. (1974). Reconnaissance of the Indian Ocean equatorial undercurrent near Addu Atoll. *Deep Sea Research and Oceanographic Abstracts*, 21, 123–129. [https://doi.org/10.1016/0011-7471\(74\)90069-2](https://doi.org/10.1016/0011-7471(74)90069-2).
- Koné, V., Aumont, O., Lévy, M., & Resplandy, L. (2009). Physical and biogeochemical controls of the phytoplankton seasonal cycle in the Indian Ocean: A modeling study. *Indian Ocean Biogeochemical Processes and Ecological Variability*, 185, 350.

- Krishnamohan, K., Vialard, J., Lengaigne, M., Masson, S., Samson, G., Pous, S., Neetu, S., Durand, F., Shenoi, S., & Madec, G. (2019). Is there an effect of Bay of Bengal salinity on the northern Indian Ocean climatological rainfall? *Deep Sea Research, Part II*, 166, 19–33.
- Kumar, S. P., Roshin, R. P., Narvekar, J., Kumar, P. D., & Vivekanandan, E. (2009). Response of the Arabian Sea to global warming and associated regional climate shift. *Marine Environmental Research*, 68(5), 217–222.
- Kwiatkowski, L., Torres, O., Bopp, L., Aumont, O., Chamberlain, M., Christian, J. R., & Ziehn, T. (2020). Twenty-first century ocean warming, acidification, deoxygenation, and upper-ocean nutrient and primary production decline from CMIP6 model projections. *Biogeosciences*, 17(13), 3439–3470.
- Lachkar, Z., Lévy, M., & Smith, S. (2018). Intensification and deepening of the Arabian Sea oxygen minimum zone in response to increase in Indian monsoon wind intensity. *Biogeosciences*, 15(1), 159–186.
- Lachkar, Z., Smith, S., Lévy, M., & Pauluis, O. (2016). Eddies reduce denitrification and compress habitats in the Arabian Sea. *Geophysical Research Letters*, 43(17), 9148–9156.
- Lau, N. C., & Nath, M. J. (2004). Coupled GCM simulation of atmosphere-ocean variability associated with zonally asymmetric SST changes in the tropical Indian Ocean. *Journal of Climate*, 17, 245–265.
- Lee, T., Fukumori, I., Menemenlis, D., Xing, Z., & Fu, L. (2002). Effects of the Indonesian throughflow on the Pacific and Indian oceans. *Journal of Physical Oceanography*, 32, 1404–1429. [https://doi.org/10.1175/1520-0485\(2002\)032<1404:EOTITO>2.0.CO;2](https://doi.org/10.1175/1520-0485(2002)032<1404:EOTITO>2.0.CO;2).
- Lee, T., & Marotzke, J. (1998). Seasonal cycles of meridional overturning and heat transport of the Indian Ocean. *Journal of Physical Oceanography*, 28, 923–943.
- Lévy, M., Resplandy, L., Palter, J. B., Couespe, D., & Lachkar, Z. (2021). The crucial contribution of mixing to present and future ocean oxygen distribution. *Ocean Mixing*, 329–344.
- Lévy, M., Shankar, D., André, J. M., Shenoi, S. S. C., Durand, F., & de Boyer Montégut, C. (2007). Basin-wide seasonal evolution of the Indian Ocean's phytoplankton blooms. *Journal of Geophysical Research: Oceans*, 112(C12).
- Li, Y., Han, W., Ravichandran, M., Wang, W., Shinoda, T., & Lee, T. (2017a). Bay of Bengal salinity stratification and Indian summer monsoon intra-seasonal oscillation: 1. Intraseasonal variability and causes. *Journal of Geophysical Research: Oceans*, 122, 4291–4311. <https://doi.org/10.1002/2017JC012691>.
- Li, Y., Han, W., Shinoda, T., Wang, C., Ravichandran, M., & Wang, J.-W. (2014). Revisiting the wintertime intraseasonal SST variability in the tropical South Indian Ocean: Impact of the ocean interannual variation. *Journal of Physical Oceanography*, 44(7), 1886–1907.
- Li, Y., Han, W., Wang, W., Ravichandran, M., Lee, T., & Shinoda, T. (2017b). Bay of Bengal salinity stratification and Indian summer monsoon intra-seasonal oscillation: 2. Impact on SST and convection. *Journal of Geophysical Research*, 122, 4312–4328. <https://doi.org/10.1002/2017JC012692>.
- Li, Y., Jourdain, N. C., Taschetto, A. S., Gupta, A. S., Argüeso, D., Masson, S., & Cai, W. (2017c). Resolution dependence of the simulated precipitation and diurnal cycle over the maritime continent. *Climate Dynamics*, 48(11–12), 4009–4028.
- Li, H., Kanamitsu, M., & Hong, S.-Y. (2012). California reanalysis downscaling at 10 km using an ocean-atmosphere coupled regional model system. *Journal of Geophysical Research – Atmospheres*, 117, D12118.
- Li, Q., Webb, A., Fox-Kemper, B., Craig, A., Danabasoglu, G., Large, W. G., & Vertenstein, M. (2016). Langmuir mixing effects on global climate: WAVEWATCH III in CESM. *Ocean Modelling*, 103, 145–160.
- Lighthill, M. J. (1969). Dynamic response of the Indian Ocean to the onset of the southwest monsoon. *Philosophical Transactions of the Royal Meteorological Society A*, A265, 45–92.
- Lu, B., Ren, H. L., Scaife, A. A., Wu, J., Dunstone, N., Smith, D., Wan, J., Eade, R., MacLachlan, C., & Gordon, M. (2018). An extreme negative Indian Ocean Dipole event in 2016: Dynamics and predictability. *Climate Dynamics*, 51, 89–100. <https://doi.org/10.1007/s00382-017-3908-2>.
- Luo, J. J., Behera, S., Masumoto, Y., Sakuma, H., & Yamagata, T. (2008). Successful prediction of the consecutive IOD in 2006 and 2007. *Geophysical Research Letters*, 35, L14S02. <https://doi.org/10.1029/2007GL032793>.
- Luo, J. J., Masson, S., Behera, S., & Yamagata, T. (2007). Experimental forecasts of the Indian Ocean dipole using a coupled OAGCM. *Journal of Climate*, 20, 2178–2190. <https://doi.org/10.1175/JCLI4132.1>.
- Luther, M., & O'Brien, J. J. (1985). A model of the seasonal circulation in the Arabian Sea forced by observed winds. *Progress in Oceanography*, 14, 353–385.
- Lutjeharms, J. R. E. (2006). *The Agulhas Current*. Springer-Verlag. ISBN 10354042392. 330 pp.
- Masson, S., Menkes, C., Delecluse, P., & Boulanger, J.-P. (2003). Impacts of salinity on the eastern Indian Ocean during the termination of the fall Wyrtki Jet. *Journal of Geophysical Research*, 108(C3), 3067. <https://doi.org/10.1029/2001JC000833>.
- Masumoto, Y., & Meyers, G. (1998). Forced Rossby waves in the southern tropical Indian Ocean. *Journal of Geophysical Research*, 103(C12), 27589–27602.
- McCreary, J. P., Kundu, P. K., & Molinari, R. L. (1993). A numerical investigation of dynamics, thermodynamics and mixed-layer processes in the Indian Ocean. *Progress in Oceanography*, 31, 181–244.
- McCreary, J. P., Kohler, K. E., Hood, R. R., & Olson, D. B. (1996). A four-component ecosystem model of biological activity in the Arabian Sea. *Progress in Oceanography*, 37(3–4), 193–240.
- McCreary, J. P., & Kundu, P. K. (1985). Western boundary circulation driven by an alongshore wind: With application to the Somali current system. *Journal of Marine Research*, 43, 493–516.
- McCreary, J. P., Yu, Z., Hood, R. R., Vinayachandran, P. N., Furue, R., Ishida, A., & Richards, K. J. (2013). Dynamics of the Indian-Ocean oxygen minimum zones. *Progress in Oceanography*, 112, 15–37.
- McPhaden, M. J., Beal, L. M., Bhaskar, T. V. S. U., Lee, T., Nagura, M., Strutton, P. G., & Yu, L. (2024). Chapter 17: The Indian Ocean Observing System (IndOOS). In C. C. Ummenhofer, & R. R. Hood (Eds.), *The Indian Ocean and its role in the global climate system* (pp. 393–419). Amsterdam: Elsevier. <https://doi.org/10.1016/B978-0-12-822698-8.00002-0>.
- Melzer, B. A., Jensen, T. G., & Rydbeck, A. V. (2019). The life cycle and interannual variability of the Great Whirl from altimetry-based eddy tracking. *Geophysical Research Letters*, 46. <https://doi.org/10.1029/2018GL081781>.

- Menezes, V. V., Phillips, H. E., Schiller, A., Bindoff, N. L., Domingues, C. M., & Vianna, M. L. (2014). South Indian Countercurrent and associated fronts. *Journal of Geophysical Research, Oceans*, 119, 6763–6791. <https://doi.org/10.1002/2014JC010076>.
- Menezes, V. V., Phillips, H. E., Vianna, M. L., & Bindoff, N. L. (2016). Interannual variability of the South Indian Countercurrent. *Journal of Geophysical Research: Oceans*, 121(5), 3465–3487.
- Metzger, E. J., Hurlburt, H. E., Xu, X., Shriner, J. F., Gordon, A. L., Sprintall, J., Susanto, R. D., & van Aken, H. M. (2010). Simulated and observed circulation in the Indonesian Seas: 1/12° global HYCOM and the INSTANT observations. *Dynamics of Atmospheres and Oceans*, 50, 275–300. <https://doi.org/10.1016/j.dynatmoce.2010.04.002>.
- Miller, A. J., Collins, M., Gualdi, S., Jensen, T. G., Misra, V., Pezzi, L. P., Pierce, D. W., Putrasahan, D., Seo, H., & Tseng, Y.-H. (2017). Coupled ocean-atmosphere-hydrology modeling and predictions. *Journal of Marine Research*, 75, 361–402.
- Misra, V., Mishra, A., & Bhardwaj, A. (2017). High-resolution regional-coupled ocean-atmosphere simulation of the Indian summer monsoon. *International Journal of Climatology*, 37, 717–740.
- Misra, V., Mishra, A., & Bhardwaj, A. (2018). Simulation of the intraseasonal variations of the Indian summer monsoon in a regional coupled ocean—Atmosphere model. *Journal of Climate*, 31(8), 3167–3185.
- Murtugudde, R., & Busalacchi, A. J. (1999). Interannual variability of the dynamics and thermodynamics of the tropical Indian Ocean. *Journal of Climate*, 12, 2300–2326.
- Nagura, M., & McPhaden, M. J. (2010). Wyrtki Jet dynamics: Seasonal variability. *Journal of Geophysical Research*, 115, C07009. <https://doi.org/10.1029/2009JC005922>.
- Nagura, M., & McPhaden, M. J. (2018). The shallow overturning circulation in the Indian Ocean. *Journal of Physical Oceanography*, 48, 413–434.
- Nyadri, E., Jensen, T. G., Richman, J., & Shriner, J. (2017). On the interactions between wind, SST and the subsurface ocean in the southwestern Indian Ocean. *IEEE Geoscience and Remote Sensing Letters*, 14(12), 2315–2319.
- Ogata, T., & Masumoto, Y. (2010). Interactions between mesoscale eddy variability and Indian Ocean dipole events in the southeastern tropical Indian Ocean—Case studies for 1994 and 1997/1998. *Ocean Dynamics*, 60, 717–730.
- Paulmier, A., & Ruiz-Pino, D. (2009). Oxygen minimum zones (OMZs) in the modern ocean. *Progress in Oceanography*, 80(3–4), 113–128.
- Pearce, A. F., & Feng, M. (2013). The rise and fall of the “marine heat wave” off Western Australia during the summer of 2010/2011. *Journal of Marine System*, 111–112, 139–156. <https://doi.org/10.1016/j.jmarsys.2012.10.009>.
- Phillips, H. E., Menezes, V. V., Nagura, M., McPhaden, M. J., Vinayachandran, P. N., & Beal, L. M. (2024). Chapter 8: Indian Ocean circulation. In C. C. Ummenhofer, & R. R. Hood (Eds.), *The Indian Ocean and its role in the global climate system* (pp. 169–203). Amsterdam: Elsevier. <https://doi.org/10.1016/B978-0-12-822698-8.00012-3>.
- Pianezze, J., Barthe, C., Bielli, S., Tulet, P., Jullien, S., Cambon, G., et al. (2018). A new coupled ocean-waves-atmosphere model designed for tropical storm studies: Example of tropical cyclone Bejisa (2013–2014) in the South-West Indian Ocean. *Journal of Advances in Modeling Earth Systems*, 10.
- Prasad, T. G., & McClean, J. L. (2004). Mechanisms for anomalous warming in the western Indian Ocean during dipole mode events. *Journal of Geophysical Research*, 109, C02019. <https://doi.org/10.1029/2003JC001872>.
- Prasanna Kumar, S., Muraleedharan, P. M., Prasad, T. G., Gauns, M., Ramaiah, N., De Souza, S. N., & Madhupratap, M. (2002). Why is the Bay of Bengal less productive during summer monsoon compared to the Arabian Sea? *Geophysical Research Letters*, 29(24).
- Quadfasel, D. (1982). Low frequency variability of the 20°C isotherm topography in the western equatorial Indian Ocean. *Journal of Geophysical Research*, 87(C3), 1990–1996.
- Rahman, H., et al. (2020). An assessment of the Indian Ocean mean state and seasonal cycle in a suite of interannual CORE-II simulations. *Ocean Modelling*, 145, 101503.
- Ramachandran, S., Tandon, A., Mackinnon, J., Lucas, A. J., Pinkel, R., Waterhouse, A. F., Nash, J., Shroyer, E., Mahadevan, A., Weller, R. A., & Farrar, J. T. (2018). Submesoscale processes at shallow salinity fronts in the Bay of Bengal: Observations during the winter monsoon. *Journal of Physical Oceanography*, 48(3), 479–509.
- Rao, S. A., Masson, S., Luo, J. J., Behera, S. K., & Yamagata, T. (2007). Termination of Indian Ocean dipole events in a coupled general circulation model. *Journal of Climate*, 20, 3018–3035. <https://doi.org/10.1175/JCLI4164.1>.
- Renault, L., Masson, S., Oerder, V., Jullien, S., & Colas, F. (2019). Disentangling the mesoscale ocean-atmosphere interactions. *Journal of Geophysical Research: Oceans*, 124, 2164–2178.
- Renault, L., McWilliams, J. C., & Penven, P. (2017). Modulation of the Agulhas Current retroflection and leakage by oceanic current interaction with the atmosphere in coupled simulations. *Journal of Physical Oceanography*, 47, 2077–2100. <https://doi.org/10.1175/JPO-D-16-0168.1>.
- Renault, L., Molemaker, M. J., Gula, J., Masson, S., & McWilliams, J. C. (2016). Control and stabilization of the Gulf stream by oceanic current interaction with the atmosphere. *Journal of Physical Oceanography*, 46(11), 3439–3453.
- Reppin, J., Schott, F. A., Fischer, J., & Quadfasel, D. (1999). Equatorial currents and transports in the upper central Indian Ocean: Annual cycle and interannual variability. *Journal of Geophysical Research*, 104, 15495–15514. <https://doi.org/10.1029/1999JC900093>.
- Resplandy, L. (2018). Will ocean zones with low oxygen levels expand or shrink? *Nature*, 557.
- Resplandy, L., Lévy, M., Bopp, L., Echevin, V., Pous, S., Sarma, V. V. S. S., & Kumar, D. (2012). Controlling factors of the oxygen balance in the Arabian Sea's OMZ. *Biogeosciences*, 9(12), 5095–5109.
- Resplandy, L., Lévy, M., Madec, G., Pous, S., Aumont, O., & Kumar, D. (2011). Contribution of mesoscale processes to nutrient budgets in the Arabian Sea. *Journal of Geophysical Research: Oceans*, 116(C11).

- Resplandy, L., Vialard, J., Lévy, M., Aumont, O., & Dandonneau, Y. (2009). Seasonal and intraseasonal biogeochemical variability in the thermocline ridge of the southern tropical Indian Ocean. *Journal of Geophysical Research: Oceans*, 114(C7).
- Roxy, M. K., Modi, A., Murtugudde, R., Valsala, V., Panickal, S., Prasanna Kumar, S., & Lévy, M. (2016). A reduction in marine primary productivity driven by rapid warming over the tropical Indian Ocean. *Geophysical Research Letters*, 43(2), 826–833.
- Roxy, M. K., Ritika, K., Terray, P., & Masson, S. (2014). The curious case of Indian Ocean warming. *Journal of Climate*, 27(22), 8501–8509.
- Roxy, M. K., Saranya, J. S., Modi, A., Anusree, A., Cai, W., Resplandy, L., ... Frölicher, T. L. (2024). Chapter 20: Future projections for the tropical Indian Ocean. In C. C. Ummenhofer, & R. R. Hood (Eds.), *The Indian Ocean and its role in the global climate system* (pp. 469–482). Amsterdam: Elsevier. <https://doi.org/10.1016/B978-0-12-822698-8.00004-4>.
- Ruppert, J. H., & Johnson, R. H. (2015). Diurnally modulated cumulus moistening in the preonset stage of the Madden–Julian oscillation during DYNAMO. *Journal of the Atmospheric Sciences*, 72(4), 1622–1647. <https://doi.org/10.1175/JAS-D-14-0218.1>.
- Ryabchenko, V. A., Gorchakov, V. A., & Fasham, M. J. R. (1998). Seasonal dynamics and biological productivity in the Arabian Sea Euphotic Zone as simulated by a three-dimensional ecosystem model. *Global Biogeochemical Cycles*, 12(3), 501–530.
- Saji, N. H., Goswami, B. N., Vinayachandran, P. N., & Yamagata, T. (1999). A dipole mode in the tropical Indian Ocean. *Nature*, 401, 360–363.
- Saji, N. H., Xie, S.-P., & Tam, C.-Y. (2006). Satellite observations of intense intraseasonal cooling events in the tropical south Indian Ocean. *Geophysical Research Letters*, 33, L14704. <https://doi.org/10.1029/2006GL026525>.
- Samson, G., Masson, S., Lengaigne, M., Keerthi, M. G., Vialard, J., Pous, S., Madec, G., Jourdain, N., Julien, S., Menkes, C., & Marchesiello, P. (2014). The NOW regional coupled model: Application to the tropical Indian Ocean climate and tropical cyclone activity. *Journal of Advances in Modeling Earth Systems*, 06. <https://doi.org/10.1002/2014MS000324>.
- Sarma, V. V. S. S., & Udaya Bhaskar, T. V. S. (2018). Ventilation of oxygen to oxygen minimum zone due to anticyclonic eddies in the Bay of Bengal. *Journal of Geophysical Research: Biogeosciences*, 123(7), 2145–2153.
- Sasaki, H., Kida, S., Furue, R., Nonaka, M., & Masumoto, Y. (2018). An increase of the Indonesian Throughflow by internal tidal mixing in a high-resolution Quasi-Global Ocean simulation. *Geophysical Research Letters*, 45, 8416–8424.
- Schiller, A., Godfrey, J. S., McIntosh, P. C., Meyers, G., & Wijffels, S. E. (1998). Seasonal near-surface dynamics and thermodynamics of the Indian Ocean and Indonesian throughflow in a global ocean general circulation model. *Journal of Physical Oceanography*, 2288–2312. [https://doi.org/10.1175/1520-0485\(1998\)028<2288:SNSDAT>2.0.CO;2](https://doi.org/10.1175/1520-0485(1998)028<2288:SNSDAT>2.0.CO;2).
- Schott, F. A., & McCreary, J. P. (2001). The monsoon circulation of the Indian Ocean. *Progress in Oceanography*, 51, 1–123.
- Schott, F. A., Swallow, J. C., & Fieux, M. (1990). The Somali Current at the equator: Annual cycle of currents and transports in the upper 1000 m and connection to neighbouring latitudes. *Deep Sea Research Part A*, 37(12), 1825–1848. [https://doi.org/10.1016/0198-0149\(90\)90080-F](https://doi.org/10.1016/0198-0149(90)90080-F).
- Schrum, C. (2017). Regional climate modeling and air-sea coupling. In *Oxford research encyclopedia of climate science*. From: <https://oxfordre.com/climatescience/view/10.1093/acrefore/9780190228620.001.0001/acrefore-9780190228620-e-3>.
- Seo, H. (2017). Distinct influence of air-sea interactions mediated by mesoscale sea surface temperature and surface current in the Arabian Sea. *Journal of Climate*, 30, 8061–8079.
- Seo, H., Miller, A. J., & Norris, J. R. (2016). Eddy-wind interaction in the California current system: Dynamics and impacts. *Journal of Physical Oceanography*, 46, 439–459.
- Seo, H., Miller, A. J., & Roads, J. O. (2007). The Scripps Coupled Ocean–Atmosphere Regional (SCOAR) model, with applications in the eastern Pacific sector. *Journal of Climate*, 20, 381–402.
- Seo, H., Murtugudde, R., Jochum, M., & Miller, A. J. (2008). Modeling of mesoscale coupled ocean–atmosphere interaction and its feedback to ocean in the Western Arabian Sea. *Ocean Modelling*, 25, 120–131.
- Seo, H., Subramanian, A. C., Miller, A. J., & Cavanaugh, N. R. (2014). Coupled impacts of the diurnal cycle of sea surface temperature on the Madden–Julian Oscillation. *Journal of Climate*, 27, 8422–8443.
- Seo, H., Subramanian, A. C., Song, H., & Chowdary, J. S. (2019). Coupled effects of ocean current on wind stress in the Bay of Bengal: Eddy energetics and upper ocean stratification. *Deep-Sea Research Part II*, 168(104), 617.
- Seo, H., Xie, S.-P., Murtugudde, R., Jochum, M., & Miller, A. J. (2009). Seasonal effects of Indian Ocean freshwater forcing in a regional coupled model. *Journal of Climate*, 22, 6577–6596.
- Shenoi, S. S. C., Shankar, D., & Shetye, S. R. (2002). Differences in heat budgets of the near-surface Arabian Sea and Bay of Bengal: Implications for the summer monsoon. *Journal of Geophysical Research*, 107(C6), 3052. <https://doi.org/10.1029/2000JC000679>.
- Shi, Q., & Bourassa, M. A. (2019). Coupling ocean currents and waves with wind stress over the Gulf stream. *Remote Sensing*, 11, 1476.
- Shinoda, T. (2005). Impact of the diurnal cycle of solar radiation on intraseasonal SST variability in the western equatorial Pacific. *Journal of Climate*, 18, 2628–2636.
- Shinoda, T., Han, W., Jensen, T. G., Zamudio, L., Metzger, E. J., & Lien, R.-C. (2016). Impact of the Madden-Julian Oscillation on the Indonesian Throughflow in the Makassar Strait during the CINDY/DYNAMO field campaign. *Journal of Climate*, 29, 6085–6108. <https://doi.org/10.1175/JCLI-D-15-0711.1>.
- Shinoda, T., Han, W., Metzger, E. J., & Hurlburt, H. (2012). Seasonal variation of the Indonesian Throughflow in Makassar Strait. *Journal of Physical Oceanography*, 42, 1099–1123. <https://doi.org/10.1175/JPO-D-11-0120.1>.
- Shinoda, T., Han, W., Zamudio, L., Lien, R.-C., & Katsumata, M. (2017). Remote Ocean response to the Madden-Julian oscillation during the DYNAMO field campaign: Impact on Somali Current System and the Seychelles-Chagos thermocline ridge. *Atmosphere*, 8(9), 171.
- Shinoda, T., Pei, S., Wang, W., Fu, J. X., Lien, R.-C., Seo, H., & Soloviev, A. (2021). Climate process team: Improvement of ocean component of NOAA climate forecast system relevant to Madden-Julian oscillation simulations. *Journal of Advances in Modeling Earth Systems*, 13. <https://doi.org/10.1029/2021MS002658>.

- Small, R. J., et al. (2008). Air-sea interaction over ocean fronts and eddies. *Dynamics of Atmospheres and Oceans*, 45, 274–319.
- Smith, R. L., Huyer, A., Godfrey, J. S., & Church, J. A. (1991). The Leeuwin Current off Western Australia, 1986–1987. *Journal of Physical Oceanography*, 21, 323–345. [https://doi.org/10.1175/1520-0485\(1991\)021<0323:TLCOWA>2.0.CO;2](https://doi.org/10.1175/1520-0485(1991)021<0323:TLCOWA>2.0.CO;2).
- Soloviev, A. V., & Lukas, R. (1996). Observation of spatial variability of diurnal thermocline and rain-formed halocline in the western Pacific warm pool. *Journal of Physical Oceanography*, 26, 2529–2538.
- Song, Q., Vecchi, G. A., & Rosati, A. (2007). Indian Ocean variability in the GFDL CM2 coupled climate model. *Journal of Climate*, 20, 2895–2916.
- Song, Q., Vecchi, G. A., & Rosati, A. J. (2008). Predictability of the Indian Ocean Sea surface temperature anomalies in the GFDL coupled model. *Geophysical Research Letters*, 35, L02701. <https://doi.org/10.1029/2007GL031966>.
- Sprintall, J., Biastoch, A., Gruenburg, L. K., & Phillips, H. E. (2024). Chapter 9: Oceanic basin connections. In C. C. Ummenhofer, & R. R. Hood (Eds.), *The Indian Ocean and its role in the global climate system* (pp. 205–227). Amsterdam: Elsevier. <https://doi.org/10.1016/B978-0-12-822698-8.00003-2>.
- Sui, C.-H., Lau, K.-M., Takayabu, Y. N., & Short, D. A. (1997). Diurnal variations in tropical oceanic cumulus convection during TOGA COARE. *Journal of the Atmospheric Sciences*, 54(1990), 639–655.
- Swallow, J. (1964). Equatorial undercurrent in the western Indian Ocean. *Nature*, 204, 436–437. <https://doi.org/10.1038/204436a0>.
- Swallow, J. C., & Fieux, M. (1982). Historical evidence for two gyres in the Somali Current. *Journal of Marine Research*, 40, 747–755.
- Takaya, Y., Bidlot, J. R., Beljaars, A., & Janssen, P. A. (2010). Refinements to a prognostic scheme of skin sea surface temperature. *Journal of Geophysical Research*, 115, C06009.
- Tanizaki, C., Tozuka, T., Doi, T., & Yamagata, T. (2017). Relative importance of the processes contributing to the development of SST anomalies in the eastern pole of the Indian Ocean Dipole and its implication for predictability. *Climate Dynamics*, 49, 1289–1304. <https://doi.org/10.1007/s00382-016-3382-2>.
- Thompson, B., Gnanaseelan, C., Parekh, A., & Salvekar, P. S. (2009). A model study on oceanic processes during the Indian Ocean Dipole termination. *Meteorology and Atmospheric Physics*, 105, 17–27. <https://doi.org/10.1007/s00703-009-0033-8>.
- Thompson, B., Gnanaseelan, C., & Salvekar, P. S. (2006). Variability in the Indian Ocean circulation and salinity and its impact on SST anomalies during dipole events. *Journal of Marine Research*, 64, 853–880.
- Thoppil, P. G., Richman, J. G., & Hogan, P. J. (2011). Energetics of a global ocean circulation model compared to observations. *Geophysical Research Letters*, 38, L15607. <https://doi.org/10.1029/2011GL048347>.
- Tozuka, T., Dong, L., Han, W., Lengainge, M., & Zhang, L. (2024). Chapter 10: Decadal variability of the Indian Ocean and its predictability. In C. C. Ummenhofer, & R. R. Hood (Eds.), *The Indian Ocean and its role in the global climate system* (pp. 229–244). Amsterdam: Elsevier. <https://doi.org/10.1016/B978-0-12-822698-8.00014-7>.
- Ummenhofer, C. C., Geen, R., Denniston, R. F., & Rao, M. P. (2024a). Chapter 3: Past, present, and future of the South Asian monsoon. In C. C. Ummenhofer, & R. R. Hood (Eds.), *The Indian Ocean and its role in the global climate system* (pp. 49–78). Amsterdam: Elsevier. <https://doi.org/10.1016/B978-0-12-822698-8.00013-5>.
- Ummenhofer, C. C., Taschetto, A. S., Izumo, T., & Luo, J.-J. (2024b). Chapter 7: Impacts of the Indian Ocean on regional and global climate. In C. C. Ummenhofer, & R. R. Hood (Eds.), *The Indian Ocean and its role in the global climate system* (pp. 145–168). Amsterdam: Elsevier. <https://doi.org/10.1016/B978-0-12-822698-8.00018-4>.
- Vecchi, G. A., Xie, S.-P., & Fischer, A. S. (2004). Ocean–atmosphere covariability in the western Arabian Sea. *Journal of Climate*, 17, 1213–1224.
- Vinayachandran, P. N., Iizuka, S., & Yamagata, T. (2002a). Indian Ocean dipole mode events in an ocean general circulation model. *Deep-Sea Research Part II*, 49, 1573–1596.
- Vinayachandran, P. N., Kurian, J., & Neema, C. P. (2007). Indian Ocean response to anomalous conditions in 2006. *Geophysical Research Letters*, 34, L15602. <https://doi.org/10.1029/2007GL030194>.
- Vinayachandran, P. N., McCreary, J. P., Jr., Hood, R. R., & Kohler, K. E. (2005). A numerical investigation of the phytoplankton bloom in the Bay of Bengal during Northeast Monsoon. *Journal of Geophysical Research: Oceans*, 110(C12).
- Vinayachandran, P. N., Murty, V. S. N., & Ramesh Babu, V. (2002b). Observations of barrier layer formation in the Bay of Bengal during summer monsoon. *Journal of Geophysical Research: Oceans*, 107(C12), SRF-19.
- Vinayachandran, P. N., & Nanjundiah, R. S. (2009). Indian Ocean Sea surface salinity variations in a coupled model. *Climate Dynamics*, 33, 245–263. <https://doi.org/10.1007/s00382-008-0511-6>.
- Vinayachandran, P. N., & Saji, N. H. (2008). Mechanisms of South Indian Ocean intraseasonal cooling. *Geophysical Research Letters*, 35, L23607. <https://doi.org/10.1029/2008GL035733>.
- Vinayachandran, P. N., et al. (2018). BoBBLE: Ocean–atmosphere interaction and its impact on the South Asian Monsoon. *Bulletin of the American Meteorological Society*, 99(8), 1569–1587.
- Vincent, C. L., & Lane, T. P. (2017). A 10-year austral summer climatology of observed and modeled intraseasonal, mesoscale, and diurnal variations over the Maritime Continent. *Journal of Climate*, 30, 3807–3828.
- Wajswicz, R. C. (2004). Climate variability over the tropical Indian Ocean sector in the NSIPP seasonal forecast system. *Journal of Climate*, 17, 4783–4804.
- Wajswicz, R. C. (2005). Potential predictability of tropical Indian Ocean SST anomalies. *Geophysical Research Letters*, 32, L24702. <https://doi.org/10.1029/2005GL024169>.
- Wajswicz, R. C. (2007). Seasonal-to-interannual forecasting of tropical Indian Ocean Sea surface temperature anomalies: Potential predictability and barriers. *Journal of Climate*, 20(13), 3320–3343. <https://doi.org/10.1175/JCLI4162.1>.
- Wang, H., McClean, J. L., Talley, L. D., & Yeager, S. G. (2018). Seasonal cycle and annual reversal of the Somali Current in an eddy-resolving global ocean model. *Journal of Geophysical Research: Oceans*, 123, 6562–6580. <https://doi.org/10.1029/2018JC013975>.

- Wang, J., & Yuan, D. (2015). Roles of western and eastern boundary reflections in the interannual sea level variations during negative Indian Ocean dipole events. *Journal of Physical Oceanography*, 45, 1804–1821.
- Warner, J. C., Armstrong, B., He, R., & Zambon, J. B. (2010). Development of a coupled ocean–atmosphere–wave–sediment transport (COAWST) modeling system. *Ocean Model*, 35(3), 230–244.
- Wei, J., Malanotte-Rizzoli, P., Eltahir, E. A. B., Xue, P., & Xu, D. (2014). Coupling of a regional atmospheric model (RegCM3) and a regional ocean model (FVCOM) over the maritime continent. *Climate Dynamics*, 43(5–6), 1575–1594.
- Weller, R. A., & Anderson, S. P. (1996). Surface meteorology and air-sea fluxes in the western Equatorial Pacific warm pool during the TOGA coupled ocean–atmosphere response experiment. *Journal of Climate*, 9(8), 1959–1990. [https://doi.org/10.1175/1520-0442\(1996\)009<1959:SMAASF>2.0.CO;2](https://doi.org/10.1175/1520-0442(1996)009<1959:SMAASF>2.0.CO;2).
- Weller, R. A., Fischer, A. S., Rudnick, D. L., Eriksen, C. C., Dickey, T. D., Marra, J., Fox, C. A., & Leben, R. R. (2002). Moored observations of upper ocean response to the monsoon in the Arabian Sea during 1994–1995. *Deep Sea Research*, 49B, 2195–2230.
- Wernberg, T., Smale, D. A., Tuya, F., Thomsen, M. S., Langlois, T. J., De Bettignies, T., ... Rousseaux, C. S. (2013). An extreme climatic event alters marine ecosystem structure in a global biodiversity hotspot. *Nature Climate Change*, 3, 78–82. <https://doi.org/10.1038/nclimate1627>.
- Wiggert, J. D., Hood, R. R., Banse, K., & Kindle, J. C. (2005). Monsoon-driven biogeochemical processes in the Arabian Sea. *Progress in Oceanography*, 65(2–4), 176–213.
- Wiggert, J. D., & Murtugudde, R. G. (2007). The sensitivity of the southwest monsoon phytoplankton bloom to variations in eolian iron deposition over the Arabian Sea. *Journal of Geophysical Research: Oceans*, 112(C5).
- Wiggert, J. D., Murtugudde, R. G., & Christian, J. R. (2006). Annual ecosystem variability in the tropical Indian Ocean: Results of a coupled bio-physical ocean general circulation model. *Deep Sea Research Part II: Topical Studies in Oceanography*, 53(5–7), 644–676.
- Wijesekara, H. W., et al. (2016). ASIRI an ocean–atmosphere initiative for Bay of Bengal. *Bulletin of the American Meteorological Society*, 97, 1859–1884.
- Wyrtki, K. (1973). An equatorial jet in the Indian Ocean. *Science*, 181, 262–264.
- Xie, S. P., Annamalai, H., Schott, F. A., & McCreary, J. P. (2002). Structure and mechanisms of South Indian Ocean climate variability. *Journal of Climate*, 15, 864–878.
- Xue, P., Malanotte-Rizzoli, P., Wei, J., & Eltahir, E. A. B. (2020). Coupled ocean–atmosphere modeling over the maritime continent: A review. *Journal of Geophysical Research, Oceans*, 125, e2019JC014978.
- Yamagata, T., Behera, S., Doi, T., Luo, J.-J., Morioka, Y., & Tozuka, T. (2024). Chapter 5: Climate phenomena of the Indian Ocean. In C. C. Ummenhofer, & R. R. Hood (Eds.), *The Indian Ocean and its role in the global climate system* (pp. 103–119). Amsterdam: Elsevier. <https://doi.org/10.1016/B978-0-12-822698-8.00009-3>.
- Yang, Y., Xie, S. P., Wu, L., Kosaka, Y., Lau, N. C., & Vecchi, G. A. (2015). Seasonality and predictability of the Indian Ocean dipole mode: ENSO forcing and internal variability. *Journal of Climate*, 28, 8021–8036. <https://doi.org/10.1175/JCLI-D-15-0078.1>.
- Yao, Z., Tang, Y., Chen, D., Zhou, L., Li, X., Lian, T., & Ul Islam, S. (2016). Assessment of the simulation of Indian Ocean Dipole in the CESM—Impacts of atmospheric physics and model resolution. *Journal of Advances in Modeling Earth Systems*, 8, 1932–1952. <https://doi.org/10.1002/2016MS000700>.
- Yokoi, T., Tozuka, T., & Yamagata, T. (2008). Seasonal variation of the Seychelles Dome. *Journal of Climate*, 21, 3740–3754.
- Yoneyama, K., & Zhang, C. (2020). Years of the maritime continent. *Geophysical Research Letters*, 47, e2020GL087182.
- Yoshida, K. (1959). A theory of the Cromwell current (the equatorial undercurrent) and of the equatorial upwelling—An interpretation in a similarity to a coastal circulation. *Journal of the Oceanographic Society of Japan*, 15, 159–170.
- Yu, L. (2019). Global air–sea fluxes of heat, fresh water, and momentum: Energy budget closure and unanswered questions. *Annual Review of Marine Science*, 11(1), 227–248. <https://doi.org/10.1146/annurev-marine-010816-060704>.
- Yu, Z., & McCreary, J. P. (2004). Assessing precipitation products in the Indian Ocean using an ocean model. *Journal of Geophysical Research, Oceans*, 109, C05013. <https://doi.org/10.1029/2003JC002106>.
- Yuan, X., Ummenhofer, C. C., Seo, H., & Su, Z. (2020). Relative contributions of heat flux and wind stress on the spatiotemporal upper-ocean variability in the tropical Indian Ocean. *Environmental Research Letters*, 15, 084047.
- Zhao, N., & Nasuno, T. (2020). How does the air-sea coupling frequency affect convection during the MJO passage? *Journal of Advances in Modeling Earth Systems*, 12, e2020MS002058.